Solving Parametric Fractional Differential Equations Arising from the Rough Heston Model using Quasi-Linearization and Spectral Collocation

Maryam Vahid Dastgerdi, Ali Foroush Bastani

Department of Mathematics, Institute for Advanced Studies in Basic Sciences, P.O. Box 45195-1159, Zanjan, Iran

Abstract

The rough Heston model has recently attracted the attention of many finance practitioners and researchers as it maintains the basic structure of the classical Heston model while having descriptive capabilities in terms of micro-structural foundations of the market. Using the fact that the characteristic function of log-price in this model could be expressed in terms of the solution of a nonlinear parametric fractional Riccati differential equation not admitting a closed-form solution, devising efficient numerical schemes for pricing and calibration under this model has become a crucial need in the computational finance community. Although the fractional Adams method has been used in most of the recent studies on the rough Heston model, this method suffers from some stability and convergence issues in treating the problem. In this paper, we present a numerical method based on Newton-Kantorovich quasi-linearization to solve the nonlinearity issue followed by spectral collocation based on "poly-fractonomials" to approximate the fractional derivative in an accurate and efficient manner. We provide sufficient conditions under which our method is convergent and the order of convergence is also obtained. In order to guarantee the specified convergence rate, we first prove some regularity results on the linearized problem and then employ the proposed scheme to solve a practical calibration problem from the SPX options market. The efficiency of the proposed method is illustrated by comparing the obtained results with those of the fractional Adams method as well as a fast hybrid scheme based on fractional power series expansion.

Keywords: Rough Heston model, Fractional nonlinear Riccati differential equation, Spectral collocation, Newton-Kantorovich quasi-linearization.
2010 MSC: 91B25, 91G60, 91G20, 34A08, 34A34

1. Introduction

The recent decade has seen a phenomenal growth in the number and variety of stochastic models for price fluctuations of financial assets. Most of these models are able to capture features like time-varying volatility, dynamic fat-tailed distributions and leverage effect very efficiently. Among them, those with explicit characteristic functions for the log-price relative are of special interest to finance practitioners and academia as they will result in efficient option pricing and calibration procedures [9, 46].

Continuous-time stochastic volatility (SV) models are among the flexible and widely used parametric asset price models in which the volatility process follows a stochastic differential equation driven by Brownian motion (see e.g. [25, 28, 43] for a review). However, empirical studies of market data show that both

*Corresponding author
Email addresses: mvahid@iasbs.ac.ir (Maryam Vahid Dastgerdi), bastani@iasbs.ac.ir (Ali Foroush Bastani)

historical and implied volatility time series display characteristics reminiscent of a fractional Brownian motion (fBm) rather than a random walk process (see e.g. [11]). In this regard, the family of rough fractional stochastic volatility (RFSV) models [29, 20] were introduced into the field with the aim of overcoming the limitations of the classical SV models in describing the term structure of volatility smiles [10, 11].

The use of fractional calculus in financial and economic modeling is not that new (see e.g. [3] for a comprehensive overview on the application of fractional tools in modeling long-memory processes, asset return distributions and option prices in the econometrics literature). The fractional stochastic volatility models were proposed in the late 1980's where the volatility was driven by a fractional Brownian motion with a Hurst parameter, $H \in (0.5, 1)$ [13, 45]. Also, a variety of research is conducted recently on the fractional Black-Scholes models [12, 8]. In a recent contribution, the family of affine Volterra processes was introduced as solutions of certain stochastic convolution equations with affine coefficients which generalize the rough volatility models (see e.g. [38]). There exists also some efforts to enhance the flexibility of these models with a local volatility component [40].

The "roughness" of the RFSV models stems from the fact that the Hurst index of the fBm driver is less than 0.5 and so the sample paths of the log-volatility process behave more chaotically than the Brownian motion. These models have attracted a considerable attention recently and many researchers are now involved in modeling, pricing, hedging, portfolio optimization and Monte-Carlo simulation under this family of models (see e.g. [26, 18, 6, 27, 39, 56, 19, 36, 54, 42, 23, 24, 30]) as well as studying their asymptotic properties [21, 31, 33].

In a recent contribution, El Euch and Rosenbaum [20] found the characteristic function of the log-price increments in the rough Heston model using the connection between nearly unstable heavy-tailed Hawkes processes and fractional volatility models[1]. Similar to the classical Heston model [35] in which the characteristic function is expressible as the solution of a Riccati differential equation, El Euch and Rosenbaum [20] showed that the characteristic function of the rough Heston model exhibits the same structure and could be expressed in terms of the solution of a fractional Riccati ordinary differential equation (FRODE).

In order to apply the rough Heston model in practice, it is necessary to calibrate it to liquidly traded plain-vanilla European options by minimizing an error criteria defined as the square root of the differences between the model prices[2] and the corresponding market quotes (see e.g. [19] for more details). Since by numerical approximation of the solution of the above mentioned FRODE we have the characteristic function of the log-price at hand, the choice of a suitable nonlinear fractional ODE solver has a profound effect on the viability of the overall procedure in terms of speed, stability and accuracy.

Among the existing numerical approaches for solving fractional differential equations, those based on finite differences [51, 15, 48, 16, 68], finite elements [70, 53] and spectral methods [64, 66, 61, 41] have gained much popularity in recent years. There exist other schemes to solve nonlinear fractional ODEs such as B-Spline collocation [41] which result in a system of nonlinear equations (see e.g. [50, 4] for an overview of numerical methods for general fractional ODEs). Due to the non-local and weakly singular nature of the fractional differential operator, the computational costs and storage requirements of numerical methods for FODEs are higher than their integer-order counterparts [50].

The fractional Adams method (see e.g. [15, 48, 16]) as a widely-used difference-based scheme is a predictor corrector type method based on Volterra integral equation formulation of the fractional ODE

[1]Taking a different approach through the theory of finite-dimensional deterministic convolution equations, Abi Jaber, et al. [38] proved that, under specific conditions on the kernel function and the coefficients of the equation, the affine Volterra processes and their corresponding Riccati-Volterra equations have a unique global solution. In particular, they show that the rough Heston model has a unique solution and its characteristic function is determined in terms of the unique solution of its associated fractional Riccati equation.

[2]Implied volatilities could also be used in the calibration process.

which is derived from applying a fractional Euler method in the predictor step followed by a fractional trapezoidal formula in its correction step. El Euch and Rosenbaum [20] and El Euch, et al. [19] employed this scheme in their numerical experiments concerning the computation of the at-the-money skew under the rough Heston model. This method while being easily implementable and having a super-linear rate of convergence, appears not to be a good candidate to solve FRODEs appearing in the rough Heston model (see Section 3). Recent research by Gatheral and Radoičić [30] shows also that in the Adams method, "... a large number of steps and computation time is required to achieve satisfactory accuracy". They conclude that "... such numerical solutions are inevitably much slower to compute than the closed-form classical Heston expression."

The failure of the Adams method is due mainly to the fact that the solution of this FRODE depends on a critical parameter and the Adams method fails to produce reliable results when applied to the problem with large parameter values due to a sharp transient behavior of the solution in this case. The problem could be partially resolved by adjusting the step-size of the base grid to the parameter used. However, this will result in a very fine grid for some parameter values and this in turn will slow-down the process considerably. Moreover, during the calibration procedure, we don't have any control on the intermediate parameter values that the optimization algorithm produces and there is no straightforward formula which relates the proper step-size to the model parameters.

In order to circumvent the above mentioned limitations of the fractional Adams method, Gatheral and Radoičić [30] proposed a rational approximation of the fractional Riccati solution, based on Padé approximants and valid in a region of its domain relevant to option valuation. Callegaro et al. [32] also studied the radius of convergence of a specific short-time series expansion and applied Richardson-Romberg extrapolation (outside the convergence domain) to obtain a "promising and encouraging" hybrid numerical scheme for all times.

In this paper, we propose an alternative computational scheme for solving FODEs based on iterative quasi-linearization (also called Newton-Kantorovich iteration) followed by spectral collocation to solve the resulting linear FODE at each iteration using fractional (non-polynomial) *Jacobi poly-fractonomials*. Quasi-linearization is a powerful nonperturbative approximation technique to solve highly nonlinear ordinary and partial differential equations which produces a rapidly convergent sequence of iterations (see e.g [7, 44]). On the other hand, (orthogonal) poly-fractonomials as solutions to (regular) fractional Sturm-Liouville eigen-problems are natural candidates to be used as basis functions for expanding the solution of FODEs. It is a well-known fact that spectral methods are "infinite-order accurate" if the expansion functions are properly chosen [22]. The complete theory of these bases could be found in [62] and other related works (see e.g. [63, 64, 67, 69]).

The proposed scheme combines the generality of quasi-linearization with the accuracy of spectral collocation to approximate the fractional derivative operator of any order using a global spectral expansion. Other advantages of the proposed numerical scheme could be summarized as follows:

(i) avoiding the numerical solution of systems of nonlinear equations;

(ii) allowing the calculation of collocation matrices for the solution and its fractional derivative only once inside the calibration process and the Newton iterations;

(iii) producing well-conditioned matrices;

(iv) availability of the numerical analysis for the scheme.

In order to ensure the validity of the proposed method and to guarantee the specified convergence rate, we first prove some regularity results on the linearized problem arising from the FRODE and then employ

the proposed scheme to solve a practical calibration problem from the SPX options market in which we use the implied volatility of the index options to measure the accuracy of fitting process. The obtained results confirm the efficiency and stability of the pricing engine which is based on the new FRODE solver. Comparisons with the Adams method show that the time and memory requirements scale suitably with increasing the number of option contracts.

We organize the rest of the paper as follow. In Section 2, the rough Heston model is briefly reviewed. Section 3 discusses the fractional Adams method and its shortcomings in solving the fractional Riccati differential equation appearing in the characteristic function of the log-price in the rough Heston model. The alternative numerical method to solve this problem and its error analysis are introduced and discussed in Sections 4 and 5. Finally, as an illustration of the efficiency of the method, option pricing and calibration of the rough Heston model is presented in Section 5. We conclude the paper with some final remarks and open questions for future research in Section 7.

2. The Rough Heston Model

We are concerned in the remainder with the rough fractional Heston model describing the coupled dynamics of the underlying asset, S, and the volatility, V, by

$$\begin{aligned} dS_t &= S_t\sqrt{V_t}dW_t, \quad S_0 = s_0 \in \mathbb{R}_+, \\ V_t &= V_0 + \frac{1}{\Gamma(\alpha)}\int_0^t (t-s)^{\alpha-1}\lambda(\theta - V_s)ds + \frac{1}{\Gamma(\alpha)}\int_0^t (t-s)^{\alpha-1}\lambda\nu\sqrt{V_s}dB_s, \quad V_0 \in \mathbb{R}_+, \end{aligned}$$

in which λ, θ, V_0 and ν are some positive constants, $\{W_t; t \geq 0\}$ and $\{B_t; t \geq 0\}$ are two correlated Brownian motions with $\langle dW_t, dB_t\rangle = \rho dt$ and $\alpha \in (1/2, 1)$ is a parameter determining the smoothness of the volatility sample paths (see [20] for more details). This model benefits from all the advantages of the classical Heston model while being interpretable in terms of the micro-structural foundations of the market[3].

It is shown (see e.g. [20]) that, for $-1/\sqrt{2} < \rho < 0$, the characteristic function of the log-price, $X_t = \log(S_t/S_0)$, is given by

$$\psi(a,t) := \mathbb{E}[e^{iaX_t}] = \exp\left[\theta\lambda I^1 h(a,t) + V_0 I^{1-\alpha} h(a,t)\right], \quad \forall t > 0, \tag{1}$$

in which $h(a,t)$ solves the following fractional Riccati differential equation:

$$D^\alpha h(a,t) = \frac{1}{2}(-a^2 - ia) + \lambda(ia\rho\nu - 1)h(a,t) + \frac{(\lambda\nu)^2}{2}h^2(a,t), \quad t \in [0,T], \tag{2}$$

$$I^{1-\alpha}h(a,0) = 0. \tag{3}$$

In (2) and (3), D^r and I^r denote, respectively, the Riemann-Liouville fractional order derivative and integral operators (see e.g. [4]) of order $r \in (0,1)$, defined by

$$\begin{aligned} D^r f(t) &= \frac{1}{\Gamma(1-r)}\frac{d}{dt}\int_0^t (t-s)^{-r} f(s)ds, \\ I^r f(t) &= \frac{1}{\Gamma(r)}\int_0^t (t-s)^{r-1} f(s)ds. \end{aligned}$$

[3] More precisely, assuming a high degree of endogeneity of market structure, absence of arbitrage opportunities, buying/selling asymmetry and presence of meta-orders as the main futures of the market micro-structure, El Euch et al. [18] arrived at the rough Heston model which exhibits both leverage effect and rough volatility.

The existence and uniqueness of a continuous solution to (2)-(3) is studied in [20] and [38].

The FRODE (2)-(3) has two main features. First, it is a nonlinear complex-valued differential equation involving a fractional-order derivative operator with no known analytic closed-form solution. Second and most important, the parameter a in the equation has a profound effect on the solution behavior (see Figure 1). In fact, in order to calculate the option prices using the characteristic function, we need to find the solution numerically for values of a with large absolute values (see Section 6 for more details).

Remark 1. In order to solve the fractional Riccati differential equation (2)-(3), it is possible to work with its equivalent integral equation formulation of the form

$$h(a,t) = \frac{I^{1-\alpha}h(a,0)}{\Gamma(\alpha)t^{1-\alpha}} + \frac{1}{\Gamma(\alpha)}\int_0^t (t-s)^{\alpha-1}F(a,h(a,s))ds, \tag{4}$$

in which

$$F(a,u) = \frac{1}{2}(-a^2-ia) + \lambda(ia\rho\nu-1)u + \frac{(\lambda\nu)^2}{2}u^2. \tag{5}$$

Note that based on condition (3), we could easily conclude that $h(a,0) = 0$. Equation (4) is a parametric second-kind nonlinear weakly singular Volterra integral equation.

Remark 2. Since the initial condition of the FRODE (2)-(3) is not given explicitly in terms of the function itself (but in terms of its Riemann-Liouville fractional integral), we could write this equation with the same right hand side but now in the language of Caputo's fractional derivative [14], defined by

$$D_*^{\alpha}u(t) = \frac{1}{\Gamma(1-\alpha)}\int_0^t (t-s)^{-\alpha}\frac{du(s)}{ds}ds,$$

and satisfying the relation

$$D_*^{\alpha}u(t) = D^{\alpha}u(t) - \frac{t^{-\alpha}}{\Gamma(1-\alpha)}u(0).$$

Since the initial condition of the fractional differential equation in the Caputo sense is given explicitly in terms of the function itself, it is usually easier to develop numerical schemes for fractional differential equations in the Caputo sense. However, it is easily seen that when the initial conditions are zero, the two problems are equivalent and so numerical as well as theoretical analysis provided for the Caputo sense fractional equation are also valid for the equation in the Riemann-Liouville sense under zero initial condition. Based on Remark 1 which implies the zero initial condition, from now on and for ease of notation, we use D^{α} interchangeably for both Caputo and Riemann-Liouville cases.

Remark 3. Note that if $h(a,t)$ solves the integral equation (4) for the function F defined in (5) and $h(a,0) = 0$, then $\widetilde{h}(a,t) := h(-ia,t)$ solves the new integral equation

$$\widetilde{h}(a,t) = \frac{1}{\Gamma(\alpha)}\int_0^t (t-s)^{\alpha-1}\widetilde{F}(a,\widetilde{h}(a,s))ds, \tag{6}$$

with

$$\widetilde{F}(a,u) = \frac{1}{2}(a^2-a) + \lambda(a\rho\nu-1)u + \frac{(\lambda\nu)^2}{2}u^2. \tag{7}$$

Based on Remark 3 which guarantees the transferability of results from one case to another, we present the numerical results in Section 3 based on the complex-valued problem (2)-(3) and the theoretical error analysis in Sections 4 and 5 based on the real-valued version (6)-(7).

3. Fractional Adams Method and its Limitations

In this section, we first briefly review the essential ideas of the fractional Adams method and then illustrate some of its limitations in solving the fractional differential equations mentioned in the previous section. This method is one of the efficient schemes to solve equation (2)-(3) and is a generalization of the one-step Adams-Bashforth-Moulton algorithm to fractional-order integral equations. Since the function F in (5) is nonlinear in its second argument, we apply a predictor-corrector algorithm to solve the problem. Detailed derivation of this method is explained in [16] and [15].

In order to briefly outline this method for solving the equation (4), consider a subdivision of the time interval $[0,T]$ into N sub-intervals of the form $[t_k, t_{k+1}]$ in which $t_k = k\Delta$, $k = 0,\cdots,N$ and $\Delta = T/N$. To simplify the notation, we define $g(t) = F(a, h(a,t))$. Taking the initial condition (3) into account, we are looking for a numerical approximation to the solution of the following equation:

$$h(a,t) = \frac{1}{\Gamma(\alpha)} \int_0^t (t-s)^{\alpha-1} g(s) ds. \tag{8}$$

The main idea is to use product trapezoidal quadrature formula to approximate the integral on the right-hand-side of (8). In other words, at any time step t_{k+1}, we apply the approximation

$$\int_0^{t_{k+1}} (t_{k+1}-s)^{\alpha-1} g(s) ds \approx \int_0^{t_{k+1}} (t_{k+1}-s)^{\alpha-1} \widetilde{g}_{k+1}(s) ds, \tag{9}$$

in which $\widetilde{g}_{k+1}$ is the piecewise linear interpolant of g with nodes and knots chosen at t_j, $0 \le j \le k+1$:

$$\widetilde{g}_{k+1}(t) = \frac{t_{j+1}-t}{t_{j+1}-t_j} g(t_j) + \frac{t-t_j}{t_{j+1}-t_j} g(t_{j+1}), \quad t \in [t_j, t_{j+1}), \quad 0 \le j \le K.$$

After some lengthy but straightforward calculation, we arrive at

$$\int_0^{t_{k+1}} (t_{k+1}-s)^{\alpha-1} \widetilde{g}_{k+1}(s) ds = \frac{\Delta^\alpha}{\alpha(\alpha+1)} \big[\sum_{j=0}^{n} a_{j,k+1} g(t_j) + g(t_{j+1}) \big]$$

in which

$$\begin{aligned} a_{0,k+1} &= k^{\alpha+1} - (k-\alpha)(k+1)^\alpha, \\ a_{j,k+1} &= (k-j+2)^{\alpha+1} + (k-j)^{\alpha+1} - 2(k-j+1)^{\alpha+1}, \quad 1 \le j \le k. \end{aligned}$$

So, the corrector formula can be written as

$$\widehat{h}_{AD}(a,t_{k+1}) = \frac{\Delta^\alpha}{\Gamma(\alpha+2)} \left[F(a, \widehat{h}^p(a,t_{k+1})) + \sum_{j=0}^{k} a_{j,k+1} F(a, \widehat{h}_{Ad}(a,t_j)) \right],$$

in which the functional equation of the Gamma function is used twice (which yields $\Gamma(\alpha)\alpha(\alpha+1) = \Gamma(\alpha+2)$). To finalize the scheme, we need the predictor formula to calculate $\widehat{h}^p(a,t_{k+1})$. To do this, we approximate the integral term in left-hand-side of (9) using the product rectangle rule as

$$\int_0^{t_{k+1}} (t_{k+1}-s)^{\alpha-1} g(s) ds \approx \frac{\Delta^\alpha}{\alpha} \sum_{j=0}^{k} b_{j,k+1} g(t_j)$$

in which

$$b_{j,k+1} = (k+1-j)^\alpha - (k-j)^\alpha, \quad 0 \le j \le k.$$

This will result in a predictor approximation for $\widehat{h}^p(a,t_{k+1}))$ of the form

$$\widehat{h}^p(a,t_{k+1}) = \frac{\Delta^\alpha}{\Gamma(\alpha+1)} \sum_{j=0}^{k} b_{j,k+1} F(a, \widehat{h}_{Ad}(a,t_j)).$$

Based on the error analysis presented in [16] (see also [48]), it could be shown that for values of $\alpha \in [0.5, 1)$, if we have $h(a,\cdot) \in C^2[0,T]$ for all $a \in \mathbb{R}$, then

$$|h(a,t_j) - \widehat{h}_{Ad}(a,t_j)| \leq C t_j^{\alpha-1} \Delta^{2-\alpha},$$

and in particular:

$$\max_{0\leq j\leq n} |h(a,t_j) - \widehat{h}_{Ad}(a,t_j)| = O(\Delta),$$

and

$$\max_{t_j \in [\varepsilon,T]} |h(a,t_j) - \widehat{h}_{Ad}(a,t_j)| = O(\Delta^{2-\alpha}),$$

for any $\varepsilon \in (0,T]$.

However, theoretical as well as numerical evidence shows that the right-hand side derivative of the solution, $h(a,t)$ w.r.t. t as $t \to 0^+$ goes to infinity, when $a \to \infty$ (see Appendix A for a theoretical explanation as well as Fig. 1 for a numerical illustration). This explains why the fractional Adams method explodes and fails to produce valid results for large values of a and returns an undefined numerical result (see Table 1).

The exploding instability of the fractional Adams method also stems from the fact that this scheme is conditionally stable (see Appendix B). As can be seen from Table 1, although refining the mesh can resolve the issue for some values of a, it just postpones the appearance of "NaN" to larger values of a. It is worth noting that this critical "large" value of a depends on the model parameters as illustrated in Fig. 2. In this figure, the cross section $\Re[h(a,1)]$ is plotted for $\alpha = 0.6$ and different values of the parameters ρ, λ, and ν. Wherever some parts of the plot are missing, the algorithm has returned undefined numerical results. We must note that the rightmost column of Table 1 shows the *mean relative error* (MRE) calculated by the relation

$$\mathrm{MRE}(N) = \frac{1}{N} \sum_{j=1}^{N} \frac{|h(a,t_j) - \widehat{h}_{\mathrm{Ad}}(a,t_j)|}{|h(a,t_j)|}. \tag{10}$$

for the fractional Adams method. Since the closed-form analytical solution of the FRODE does not exist, we have considered an approximate solution computed by the fractional Adams method with $N = 12800$ time steps as a proxy for the "exact" solution.

Based on the shortcomings of the fractional Adams method outlined above, it is natural to think about other alternative approaches to deal with FRODEs arising from rough fractional stochastic volatility models. As a first remedy, it is possible to use non-uniform grid points in the finite difference discretization using optimal mesh-sizes obtained from stability conditions of the underlying scheme. This topic deserves a separate attention in its own right and will be pursued elsewhere. The other alternative which is pursued here is based on the theory of quasi-linearization and spectral collocation which will be outlined in the remainder.

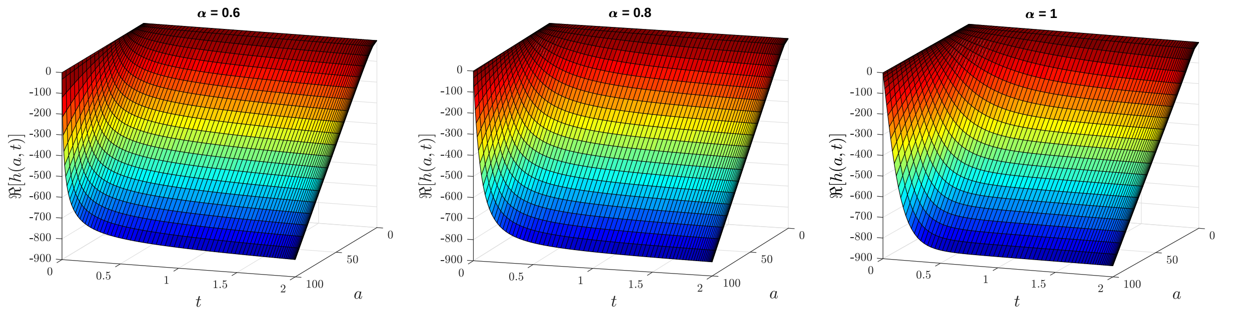

Figure 1: The solution of fractional Riccati equation for $\rho = -0.5$, $\nu = 0.5$, $\lambda = 0.2$ and different values of α.

Table 1: Approximate solution of the fractional Riccati equation (2)-(3) at $T = 2$ for parameter values $\rho = -0.5$, $\nu = 0.5$, $\lambda = 0.2$ $\alpha = 0.6$ and different values of a using the fractional Adams method. N_{Ad} is the number of time steps.

a	N_{Ad}	$\Re[\widehat{h}_{Ad}(a,T)]$	$\Im[\widehat{h}_{Ad}(a,T)]$	time (s)	MRE(N_{Ad})
10	50	-49.0659150695	14.8431562460	0.03	0.3806
	100	-49.0744759134	14.8415100884	0.04	0.1340
	200	-49.0772023771	14.8410382227	0.12	0.0486
	400	-49.0780825041	14.8408958427	0.33	0.0183
	800	-49.0783690070	14.8408514172	1.17	0.0070
	1600	-49.0784627563	14.8408372543	4.40	0.0026
	3200	-49.0784935316	14.8408326774	17.09	8.3e-04
	6400	-49.0785036544	14.8408311858	72.20	3.9e-07
	12800	-49.0785069884	14.8408306972	349.75	—
100	50	-8.21733370e+02	5.01209488e+02	0.02	0.3150
	100	-8.16142423e+02	4.63988366e+02	0.04	0.1042
	200	-8.16515723e+02	4.64180004e+02	0.08	0.0376
	400	-8.16584730e+02	4.64213767e+02	0.36	0.0138
	800	-8.16601994e+02	4.642224210e+02	1.23	0.0051
	1600	-8.16606859e+02	4.64224928e+02	4.38	0.0018
	3200	-8.16608317e+02	4.64225697e+02	17.54	5.6e-04
	6400	-8.16608769e+02	4.64225939e+02	78.16	3.7e-06
	12800	-8.16608913e+02	4.64226017e+02	327.96	—
1000	1600	NaN	NaN	—	—
	3200	-8.61056342e+03	4.96535070e+03	18.27	5.2e-04
	6400	-8.61052875e+03	4.96539020e+03	59.32	5.5e-05
	12800	-8.61053211e+03	4.96539270e+03	233.02	—
1500	3200	NaN	NaN	—	—
	6400	-1.29406708e+04	7.46541212e+03	58.22	1.8e-04
	12800	-1.29406631e+04	7.46543919e+03	230.09	—

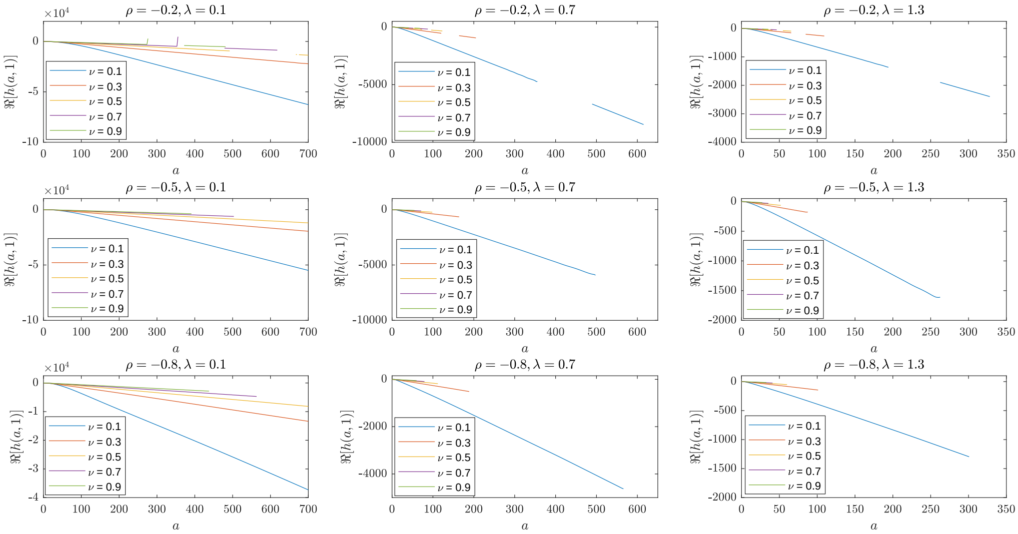

Figure 2: The fractional Adams method fails to produce valid results for large values of a for different parameter sets. Wherever some parts of the plot are missing, the algorithm has returned undefined numerical results.

4. Quasi-Linearization

In order to deal with the nonlinearity present in (2)-(3), we apply the iterative quasi-linearization (Newton-Kantorovich) scheme resulting in a linear fractional ordinary differential equation (FODE) at each step and then approximate the solution of this linearized problem using the Jacobi poly-fractonomials to cope with with the fractional derivative operator.

Let us consider the nonlinear fractional ordinary differential equation of the form

$$\begin{aligned} D^{\alpha}u(t) &= f(t,u(t)), \quad 0 \le t \le T, & (11) \\ u(0) &= u^0, & (12) \end{aligned}$$

in which the function $f \in C((0,T] \times \mathbb{R}))$ satisfies the following two assumptions:

Assumption 1. *For some $0 \le \sigma < \alpha < 1$, the two functions $t^{\sigma} f(t,x)$ and $t^{\sigma} \frac{\partial}{\partial x} f(t,x)$ belong to $C([0,T] \times \mathbb{R}))$.*

Assumption 2. *For some $0 \le \sigma < \alpha < 1$ and some $L > 0$, we have $\left| t^{\sigma} \left[\frac{\partial}{\partial x} f(t,x_1) - \frac{\partial}{\partial x} f(t,x_2) \right] \right| \le L|x_1 - x_2|$ for all $t \in [0,T]$ and $x_1, x_2 \in \mathbb{R}$.*

Remark 4. It is straightforward to verify Assumptions 1 and 2 for the fractional quadratic Riccati differential equation with $f(t,x) = c_0 + c_1 x + c_2 x^2$ for some constants c_0, c_1 and c_2. Obviously, for any $\sigma \ge 0$, $t^{\sigma} f(t,x)$ and $t^{\sigma} \frac{\partial}{\partial x} f(t,x) = t^{\sigma}(c_1 + 2c_2 x)$ belong to $C([0,T] \times \mathbb{R})$ and so the Assumption 1 is satisfied. Moreover, we have

$$\left| t^{\sigma} \left[\frac{\partial}{\partial x} f(t,x_1) - \frac{\partial}{\partial x} f(t,x_2) \right] \right| \le T^{\sigma} \left| \frac{\partial}{\partial x} f(t,x_1) - \frac{\partial}{\partial x} f(t,x_2) \right| \le 2c_2 T^{\sigma} |x_1 - x_2|,$$

for all $t \in [0,T]$ and $x_1, x_2 \in \mathbb{R}$ and so the Assumption 2 is also satisfied with $L = 2c_2 T^{\sigma}$.

Based on the fact that the function f is nonlinear in its second argument, quasi-linearization is proposed here as a suitable method to deal with the nonlinearity issue. This method introduces an iterative procedure which, starting from an initial guess, improves the solution at each iteration using the first term of the Taylor expansion of the underlying operator (see [2] for more details). In other words, the quasilinear iterative scheme is obtained by linearizing the equation around the n-th approximation by expanding the function f in a power series and retaining only the linear terms. In the case of fractional differential equation (11)-(12), it is defined by the recurrence relation

$$D^{\alpha}u_n = f(t,u_{n-1}) + f_2(t,u_{n-1})(u_n - u_{n-1}), \quad u_n(0) = u^0, \quad n = 0,1,2,\cdots, \tag{13}$$

in which $u_{n-1}(\cdot)$ and $u_n(\cdot)$ are successive approximations to the solution and $f_2(t,x) := \frac{\partial}{\partial x}f(t,x)$. We emphasize that for every $n > 0$, $u_{n-1}(\cdot)$ is known at the n-th iteration, either from the initial guess ($n = 1$) or from the previous steps ($n > 1$). Consequently, $f(t,u_{n-1})$ and $f_2(t,u_{n-1})$ are single-variable functions of time, t. Therefore, despite the presence of f and f_2, equation (13) is linear w.r.t. $u_n(\cdot)$. The procedure is summarized in Algorithm 1.

Algorithm 1 Quasi-linearization Algorithm

1: Pick an initial guess u_0 and an error tolerance ε;
2: Set $n = 0$ and $v = 1$;
3: **while** $v > \varepsilon$ **do**
4: Increase n by 1;
5: Solve the linearized problem (13):

$$(D^{\alpha} - f_2(t,u_{n-1})I)u_n = f(t,u_{n-1}) - f_2(t,u_{n-1})u_{n-1};$$

6: Update v by $v := \|u_n - u_{n-1}\|$;
7: **end while**

In the next subsection, we provide sufficient conditions on the initial guess, $u_0(\cdot)$, under which the Algorithm 1 is convergent and the rate of convergence is also derived. Moreover, an example of a suitable initial guess is provided.

4.1. Convergence Analysis of the Quasi-Linearized Iterative Process

The proposed iterative procedure (13) could be considered as an operator Newton scheme to solve the weakly-singular integral equation

$$u(t) = u^0 + \frac{1}{\Gamma(\alpha)}\int_0^t (t-s)^{\alpha-1} f(s,u(s))ds, \tag{14}$$

which is equivalent to finding the (unique) zero of the operator $\mathcal{F} : C([0,T],\mathbb{R}) \to C([0,T],\mathbb{R})$, defined by

$$(\mathcal{F}u)(t) \quad = \quad u(t) - u^0 - \frac{1}{\Gamma(\alpha)}\int_0^t (t-s)^{\alpha-1} f(s,u(s))ds. \tag{15}$$

In order to guarantee the convergence of Newton iterations to the solution of (14), we need to show that the operator $\mathcal{F}$ is Fréchet differentiable and it's Fréchet derivative, $\mathcal{F}'_u(h)$ at the point $u \in C[0,T]$, defined implicitly by the relation

$$\lim_{\|h\| \longrightarrow 0} \frac{\mathcal{F}(u+h) - \mathcal{F}(u) - \mathcal{F}'_u(h)}{\|h\|} = 0,$$

has a bounded inverse. It could be shown (see e.g. [59]) that the operator $\mathcal{F}$ defined by (15) is Fréchet differentiable everywhere and we have

$$\mathcal{F}_u' h(t) = h(t) - \frac{1}{\Gamma(\alpha)} \int_0^t (t-s)^{\alpha-1} f_2(s,u(s))h(s)ds, \quad \forall h \in C[0,T].$$

In order to ensure the quadratic rate of convergence for the iteration (13), we need the following theorem (see e.g. Vijesh [59]) which provides sufficient conditions for the global convergence of the scheme. Before presenting the result, we review some features of the problem which will be used in the sequel. Choosing a suitable value for σ satisfying Assumptions 1 and 2, we define the constants $M, \eta \in \mathbb{R}$ by

$$M = \sup_{t\in[0,T]} |t^{\sigma} f_2(t,u_0)|, \tag{16}$$

and

$$\eta = \sup_{t\in[0,T]} |\mathcal{F} u_0(t)|, \tag{17}$$

in which $u_0 \in C[0,T]$ is the starting point of the iteration and the operator $\mathcal{F}$ is given by 15. Consider now the following two assumptions:

Assumption 3. *The constant M defined in (16) satisfies the inequality*

$$\frac{\Gamma(1-\sigma)T^{\alpha-\sigma}M}{\Gamma(1+\alpha-\sigma)} < 1,$$

for some $0 \le \sigma < \alpha < 1$.

Assumption 4. *The constants M,* η *and L defined respectively in (16), (17) and Remark 4 satisfy the inequality*

$$\frac{L\Gamma(1+\alpha-\sigma)\Gamma(1-\sigma)T^{\alpha-\sigma}\eta}{(\Gamma(1+\alpha-\sigma)-\Gamma(1-\sigma)T^{\alpha-\sigma}M)^2} \le \frac{1}{4},$$

for some $0 \le \sigma < \alpha < 1$.

Theorem 1 ([59], Theorem 3.1)**.** Let $u_0(\cdot) \in C[0,T]$ and suppose that Assumptions (3) and (4) are satisfied. Then the fractional differential equation (11)-(12) has a unique solution u^* in $\overline{U}(u_0,r)$, the closed ball with center u_0 and radius r, with

$$r = \frac{2\Gamma(1+\alpha-\sigma)\eta}{\Gamma(1+\alpha-\sigma)-M\Gamma(1-\sigma)T^{\alpha-\sigma}}.$$

Furthermore, the quasilinear iterative scheme (13) starting from u_0 converges quadratically to u^* and for each $n \in \mathbb{N}$, we have

$$\|u^* - u_n\|_\infty \le C2^{-n}\theta^{2^n},$$

in which

$$\theta = \frac{4L\Gamma(1+\alpha-\sigma)\Gamma(1-\sigma)T^{\alpha-\sigma}\eta}{[\Gamma(1+\alpha-\sigma)-M\Gamma(1-\sigma)T^{\alpha-\sigma}]^2} \le 1.$$

In the above relations, C is some constant and $\|f\|_\infty = \sup_{t\in[0,T]} |f(t)|$.

Proof. Vijesh [59] stated the above theorem for the Caputo fractional derivative operator. However, his proof only depends on the integral representation of the problem, which is the same for both Caputo and Riemann-Liouville cases, up to a fractional power function of the independent variable which vanishes under zero initial condition (see Remark 2 and [14] for more details on the integral representation of FODEs). So the result is also valid for the Riemann-Liouville fractional derivative operator with a zero initial condition.

□

Remark 5. (**A Suitable Initial Starting Point**) In the case of fractional quadratic Riccati differential equation of the form

$$D^{\alpha}u = c_0 + c_1 u + c_2 u^2 =: f(t,u), \tag{18}$$

with initial condition, $u(0) = 0$, the quasilinear iterative method takes the form:

$$D^{\alpha}u_n - (c_1 + 2c_2 u_{n-1}(t))u_n = c_0 - c_2[u_{n-1}(t)]^2, \quad u_n(0) = 0. \tag{19}$$

Let us denote by $\widetilde{u}(\cdot)$ the solution of corresponding (integer-order) ordinary Riccati differential equation

$$\begin{aligned} \widetilde{u}'(t) &= f(t,\widetilde{u}(t)), \\ \widetilde{u}(0) &= 0, \end{aligned}$$

with the exact solution

$$\widetilde{u}(t) = \frac{2c_0}{\sqrt{c_1^2 - 4c_0c_2}\coth\left(\sqrt{c_1^2 - 4c_0c_2}\, t/2\right) - c_1}.$$

Now, if we define

$$\begin{aligned} \widetilde{M} &= \sup_{t\in[0,T]} |f_2(t,\widetilde{u}(t))|, \\ \widetilde{\eta} &= \sup_{t\in[0,T]} |\mathcal{F}\widetilde{u}(t)|, \end{aligned}$$

and select ε_1 and ε_2 satisfying

$$\begin{aligned} 0 &< \varepsilon_1 < \frac{\Gamma(1+\alpha)}{\widetilde{M}T^{\alpha}}, \\ 0 &< \varepsilon_2 < \frac{(\Gamma(1+\alpha) - \widetilde{M}T^{\alpha})^2}{8c_2\Gamma(1+\alpha)T^{\alpha}\widetilde{\eta}}, \end{aligned}$$

then by setting $\varepsilon = \min\{\varepsilon_1, \varepsilon_2\}$ and choosing $u_0(t) := \varepsilon\widetilde{u}(t)$, all of the conditions of Theorem 1 are satisfied by $\sigma = 0$, $M = \varepsilon\widetilde{M}$ and $\eta = \varepsilon\widetilde{\eta}$.

Based on the fact that the linearized problem (13) does not admit a closed form exact solution in the case of fractional Riccati equation, we propose a spectral collocation method to approximate $u_n(\cdot)$ numerically which will be discussed in the next section.

5. Spectral Collocation using Poly-Fractonomials

Spectral collocation methods are efficient and highly accurate numerical schemes to solve linear and nonlinear ordinary and partial differential equations (see e.g. [37] and the many references therein). They are based on the expansion of the solution in terms of some globally supported basis functions in which the expansion coefficients are obtained in such a way that the differential equation is satisfied exactly at a set of so-called collocation points. The fundamental unknowns are the solution values at these points and the most appropriate choice of collocation points is the set of Gauss-Lobatto-Chebyshev quadrature nodes based on the theory presented in e.g. [34].

The popularity of these methods stems from several advantages which they have over common finite difference methods. First, they have the potential for rapidly convergent approximations. The dual representation in physical and transform space allows for automatic monitoring of the spectrum of the solution, providing thus a check on resolution. If certain symmetries exist in the solution, spectral methods allow the exploitation of these symmetries. Finally, the methods have low or non-existent phase and dissipation errors [37].

The linearized problem (13) could now be solved using spectral collocation methods. Note that this equation contains a global fractional derivative operator, suggesting the use of global numerical approximation schemes such as spectral methods, rather than the local ones such as fractional Adams method. But still, due to the presence of the fractional derivative operator, the choice of suitable and efficient spectral basis functions is crucial. Zayernouri and Karniadakis [63] have shown that Jacobi poly-fractonomials as analytical eigen-solutions of the regular fractional Sturm-Liouville problem (RFSLP) of first kind are suitable choices with favorable properties. In their consecutive work [64], they also have introduced the shifted Jacobi poly-fractonomials and their fractional derivatives. So, we are provided with a natural basis function[4] to solve our linear fractional Riccati differential equation using a spectral collocation scheme.

5.1. Fractional Basis Functions

The employed spectral collocation method relies on Jacobi poly-fractonomials explicitly defined as

$$\mathcal{P}_n^{\mu}(x) = (x+1)^{\mu} P_{n-1}^{-\mu,\mu}(x), \quad x \in [-1,1],$$

in which $P_{n-1}^{-\mu,\mu}(x)$ is the standard Jacobi polynomial with $\mu \in (0,1)$. Recall that for $a,b > -1$, $P_k^{a,b}(\cdot)$ denotes the Jacobi polynomial of degree k which has the explicit representation

$$P_k^{a,b}(x) = \sum_{m=0}^{k} \frac{(-1)^{k-m}(1+b)_k(1+a+b)_{k+m}}{m!(k-m)!(1+b)_m(1+a+b)_k} \left(\frac{1+x}{2}\right)^m,$$

where for $\theta \in \mathbb{R}$, $(\theta)_0 = 1$ and $(\theta)_i = \theta(\theta+1)\cdots(\theta+i-1)$ for $i = 1,2,\cdots$.

Applying the affine mapping $x(t) = 2t/T - 1$ to transform $[0,T]$ into $[-1,1]$, gives us the shifted basis functions:

$$\widetilde{\mathcal{P}}_n^{\mu}(t) = \mathcal{P}_n^{\mu}(x(t)) = \left(\frac{2}{T}\right)^{\mu} t^{\mu} P_{n-1}^{-\mu,\mu}(x(t)), \quad t \in [0,T]. \tag{20}$$

Using the fractional Riemann-Liouville derivative of power functions (see e.g. [57]) of the form

$$D^{\mu}[t^{\nu}] = \frac{\Gamma(1+\nu)}{\Gamma(1+\nu-\mu)} t^{\nu-\mu}, \quad \nu > -1,$$

[4] The use of these basis functions will result in exponential error decay phenomena which is theoretically proven for general Fourier-based spectral or pseudo-spectral methods (see e.g. [22]).

the linearity of the the fractional operators and a little algebra, the fractional Riemann-Liouville derivative of the transformed function (20) could be obtained as

$$D^{\mu}[\widetilde{\mathcal{P}}_n^{\mu}(t)] = \left(\frac{2}{T}\right)^{\mu} \frac{\Gamma(n+\mu)}{\Gamma(n)} P_{n-1}(x(t)), \tag{21}$$

in which $P_k(\cdot) = P_k^{0,0}(\cdot)$ denotes the standard Legendre polynomial of degree k. This formula states that the μ-order fractional derivative of such poly-fractonomial basis functions of degree $(n-1+\mu)$ are multiples of the standard Legendre polynomials of integer degree (see [64, 65] for more details).

5.2. Problem Discretization by Collocation

The main motivation for the use of spectral methods in numerical analysis is the attractive approximation properties of orthogonal polynomial or (nonpolynomial) poly-fractonomial expansions. It is shown in [63] that Jacobi poly-fractonomials, $\{\mathcal{P}_n^{\alpha}(x)\}_{n=0}^{\infty}$, are orthogonal with dense linear span in $L^2_{-\alpha,-\alpha}[-1,1]$. As will be shown in the proof of Theorem 3, the solution, u, of the fractional Riccati equation (18) and also the solution, u_n, of the linearized problem (19), both belong to $L^2_{-\alpha,-\alpha}[0,T]$ for each n and so they could be expanded in a shifted Jacobi poly-fractonomial series on $[0,T]$ as

$$\begin{aligned} u(t) &= \sum_{j=1}^{\infty} \xi_j \widetilde{\mathcal{P}}_j^{\alpha}(t), \\ u_n(t) &= \sum_{j=1}^{\infty} \xi_{n,j} \widetilde{\mathcal{P}}_j^{\alpha}(t). \end{aligned}$$

In the above expressions, the expansion coefficients are given analytically by

$$\xi_j = \left(\frac{T}{2}\right)^{2\alpha-1} \frac{1}{C_{j-1}^{-\alpha,\alpha}} \int_0^T u(t)\omega(t)\widetilde{\mathcal{P}}_j^{\alpha}(t)dt, \tag{22}$$

$$\xi_{n,j} = \left(\frac{T}{2}\right)^{2\alpha-1} \frac{1}{C_{j-1}^{-\alpha,\alpha}} \int_0^T u_n(t)\omega(t)\widetilde{\mathcal{P}}_j^{\alpha}(t)dt, \tag{23}$$

where the weight function is given by $\omega(t) = (T-t)^{-\alpha}t^{-\alpha}$ and the orthogonality constant, $C_j^{-\alpha,\alpha}$, is defined by

$$C_j^{-\alpha,-\alpha} = \|P_j^{-\alpha,\alpha}\|^2_{L^2_{-\alpha,\alpha}} = \int_{-1}^{1} (1-x)^a(1+x)^b \left(P_j^{-\alpha,\alpha}(x)\right)^2 dx.$$

It is well known that the magnitude of the expansion coefficients (22) and (23) will depend only on the degree of smoothness of the solution. In particular, if u and u_n are infinitely differentiable, then the ξ_j and $\xi_{n,j}$ will decay faster than any polynomial of $1/j$.

Among the many different ways to approximate the solution of (13) by a finite-term expansion, the spectral collocation method is based on finding an approximation $\widehat{u}_{n,N}(\cdot)$ to $u_n(\cdot)$ belonging to

$$\mathcal{V}_N^{\mu} = \{v | v = t^{\mu}\pi, \quad \pi \in \mathbb{P}_N([0,T])\},$$

in which $\mathbb{P}_N([a,b])$ is the space of all algebraic polynomials of degree up to N defined on the interval $[a,b]$. Choosing the shifted Jacobi poly-fractonomials as a base for $\mathcal{V}_N^{\mu}$ and setting $\mu = \alpha$, the function $\widehat{u}_{n,N}(\cdot)$ and

its fractional derivative could be expanded as

$$\widehat{u}_{n,N}(t) = \sum_{j=1}^{N+1} \widehat{\xi}_{n,j} \widetilde{\mathcal{P}}_j^{\alpha}(t), \tag{24}$$

$$D^{\alpha}[\widehat{u}_{n,N}(t)] = \sum_{j=1}^{N+1} \widehat{\xi}_{n,j} D^{\alpha}[\widetilde{\mathcal{P}}_j^{\alpha}(t)], \tag{25}$$

in which $D^{\alpha}[\widetilde{\mathcal{P}}_j^{\alpha}(t)]$ is given by equation (21).

As our collocation points, we use the shifted Gauss-Lobatto-Chebyshev quadrature nodes in the interval $[0,T]$ given by

$$t_j = \frac{T}{2}(x_j + 1), \quad j = 1, 2, \cdots, N+1, \tag{26}$$

in which the x_j's are the standard Gauss-Lobatto-Chebyshev nodes defined by

$$x_j = \cos\Big(\frac{\pi}{2}\frac{2j-1}{N+1}\Big), \quad j = 1, \cdots, N+1.$$

Inserting the expansion (25) into the equation (13) and collocating the result at the nodes (26), the problem of finding the approximation, $\widehat{u}_{n,N}(.)$ will be transformed into finding the coefficients $\widehat{\xi}_{n,j}$ which satisfy the linear system of equations of the form

$$[D - F_{n-1}^{(2)} P]\widehat{\xi}_n = b_{n-1}. \tag{27}$$

In the above equation, we have

$$\begin{aligned}
\widehat{\xi}_n &= \begin{pmatrix} \widehat{\xi}_{n,1} \\ \vdots \\ \widehat{\xi}_{n,N+1} \end{pmatrix}, \\
P &= \begin{pmatrix} \widetilde{\mathcal{P}}_1^{\alpha}(t_1) & \dots & \widetilde{\mathcal{P}}_{N+1}^{\alpha}(t_1) \\ \vdots & \ddots & \vdots \\ \widetilde{\mathcal{P}}_1^{\alpha}(t_{N+1}) & \dots & \widetilde{\mathcal{P}}_{N+1}^{\alpha}(t_{N+1}) \end{pmatrix}, \\
D &= \begin{pmatrix} D^{\alpha}[\widetilde{\mathcal{P}}_1^{\alpha}(t_1)] & \dots & D^{\alpha}[\widetilde{\mathcal{P}}_{N+1}^{\alpha}(t_1)] \\ \vdots & \ddots & \vdots \\ D^{\alpha}[\widetilde{\mathcal{P}}_1^{\alpha}(t_{N+1})] & \dots & D^{\alpha}[\widetilde{\mathcal{P}}_{N+1}^{\alpha}(t_{N+1})] \end{pmatrix}, \\
F_{n-1}^{(2)} &= \begin{pmatrix} f_2(t_1, u_{n-1}(t_1)) & 0 & \dots & 0 \\ \vdots & & \ddots & \vdots \\ 0 & \dots & 0 & f_2(t_{N+1}, u_{n-1}(t_{N+1})) \end{pmatrix}, \\
b_{n-1} &= \begin{pmatrix} f(t_1, u_{n-1}(t_1)) - f_2(t_1, u_{n-1}(t_1))u_{n-1}(t_1) \\ \vdots \\ f(t_{N+1}, u_{n-1}(t_{N+1})) - f_2(t_{N+1}, u_{n-1}(t_{N+1}))u_{n-1}(t_{N+1}) \end{pmatrix}.
\end{aligned}$$

Our numerical procedure is now complete in the sense that we first use Algorithm 1 to convert the original nonlinear problem into a series of linear fractional differential equations trough the Newton iteration

and then we employ the fractional spectral collocation scheme (27) to solve these linearized problems at each iteration. In the remainder of this section, we present an error estimate for the fractional spectral collocation scheme (27) and the complete numerical procedure discussed above. Based on the fact that the error in spectral collocation phase decays exponentially fast as the number of expansion terms increases (see e.g. [65]), we focus only on the accuracy of Newton quasilinearization as well as projection on the space of fractonomial basis functions.

5.3. Error Analysis

In order to conduct convergence rate analysis of the approximation procedure based on the spectral expansion in (24), we use the following result from [17, Theorem 3.6] which provides an error estimate for the above spectral approximation method.

Before presenting the result, we need to introduce some notation. Let $I = [0,T]$ and define the function spaces $B^m_{\gamma,\delta}(I)$ and $\mathcal{B}^q_{\gamma,-\delta}(I)$ respectively by

$$\begin{aligned} B^m_{\gamma,\delta}(I) &:= \{u | u^{(k)} \in L^2_{\gamma+k,\delta+k}(I), k = 0,1,\cdots,m\}, \\ \mathcal{B}^q_{\gamma,-\delta}(I) &:= \{u | D^{\delta+l} u \in L^2_{\gamma+\delta+l,l}(I), l = 0,1,\cdots,q\}, \end{aligned}$$

in which $u^{(k)}$ denotes the k-order derivative of u. Let also $L^2_{\gamma,\delta}(I)$ denote the space of all functions u defined on the interval I with the corresponding norm $\|u\|_{L^2_{\gamma,\delta}(I)} < \infty$. The inner product and norm are defined as

$$\begin{aligned} (u_1,u_2)_{L^2_{\gamma,\delta}(I)} &= \int_I u_1(x) u_2(x) w^{\gamma,\delta}(x) dx, \\ \|u\|_{L^2_{\gamma,\delta}(I)} &= (u,u)^{1/2}_{L^2_{\gamma,\delta}(I)}, \end{aligned}$$

in which $w^{\gamma,\delta}(x) = (T-x)^{\gamma} x^{\delta}$ and $\gamma,\delta > -1$.

If we choose $\gamma = -\alpha$, $\delta = \alpha$, $m = 1$ and $s = 0$ in Theorem 3.6 from Duan et al. [17], we obtain the following simplified version of their result for spectral projection.

Theorem 2. Suppose for some positive integer q, that $u(\cdot) \in C(I) \cap B^1_{-\alpha,-\alpha}(I) \cap \mathcal{B}^q_{-\alpha,-\alpha}(I)$, where $\alpha \in (0,1)$ and define

$$u_N(\cdot) = \sum_{j=1}^{N+1} \xi_j \widetilde{\mathcal{P}}^{\alpha}_j(\cdot).$$

Then there exists a constant C independent of N such that for $1 < q \leq N+1$ we have

$$\|u - u_N\|_\infty \leq C N^{1-q} \left\| D^{\alpha+q} u \right\|_{L^2_{q,q}},$$

and for $q > N+1$, we have

$$\|u - u_N\|_\infty \leq C \frac{N^{1/2-\alpha}}{N!} e^{-N} \left\| D^{\alpha+1+N} u \right\|_{L^2_{N+1,N+1}}.$$

Proof. To prove the theorem, it is enough to let $\gamma = -\alpha$, $\delta = \alpha$, $m = 1$, $s = 0$ in [17, Theorem 3.6]. $\square$

Theorem 3 ensures us that the solution of the fractional Riccati equation, $u(\cdot)$, as well as the n-th Newton iteration, $u_n(\cdot)$, satisfy the conditions of Theorem 2 for $q = 2$. We will use these two theorems in Theorems 4 and 5 to obtain the convergence rate of our proposed scheme.

Theorem 3. For any positive integer n, if $u_{n-1}(\cdot) \in C(I)$, then the solution $u_n(\cdot)$ of the quasi-linearized problem (19) belongs to $C(I) \cap B^1_{-\alpha,-\alpha}(I) \cap \mathcal{B}^2_{-\alpha,-\alpha}(I)$. Moreover, the solution $u(\cdot)$ of the fractional Riccati equation (18) with zero initial condition belongs to the same space. In particular, $u \in L^2_{-\alpha,-\alpha}(I)$ and $D^{\alpha+2}u \in L^2_{2,2}(I)$.

Proof. We need to prove that at each iteration, $u_n(\cdot)$ and its derivatives satisfy the following conditions:

(i) $u_n^{(k)} \in L^2_{-\alpha+k,-\alpha+k}(I), \quad k = 0, 1,$

(ii) $D^{\alpha+l}u_n \in L^2_{l,l}(I), \quad l = 0, 1, 2.$

Note that we can rewrite equation (19) as the following Volterra integral equation:

$$u_n(t) = \frac{1}{\Gamma(\alpha)} \int_0^t (t-s)^{-(1-\alpha)} \left([c_1 + 2c_2 u_{n-1}(s)]u_n(s) + c_0 - c_2 u_{n-1}^2(s)\right) ds, \quad u^{(n)}(0) = 0.$$

It is shown in [55] that u_n is weakly singular of order one (see Appendix A), which implies that $u_n \in C[0,T] \cap C^1(0,T]$. Moreover, for every $\varepsilon > 0$, $u_n^{(1)}(t)$ is absolutely continuous on $\varepsilon \le t \le T$ and so is bounded on this interval. Similarly, being continuous on a closed interval, u_n is bounded on $[0,T]$. Let us define

$$M_0 := \sup_{0 \le t \le T} u_n(t), \quad M_1 := \sup_{\varepsilon \le t \le T} u_n^{(1)}(t).$$

Moreover, $u_n^{(1)}(t) = O(t^{\alpha-1})$, i.e. there are $\varepsilon_1, K_1 > 0$ such that $|u_n^{(1)}(t)| < K_1 t^{\alpha-1}$, $\forall 0 < t < \varepsilon_1$. So we have

$$\int_0^T (u_n(s))^2 (T-s)^{-\alpha} s^{-\alpha} ds < M_0^2 \int_0^T (T-s)^{-\alpha} s^{-\alpha} ds \;=\; M_0^2 \,\frac{T^{1-2\alpha}\Gamma(1-\alpha)^2}{\Gamma(2-2\alpha)} < \infty,$$

and so $u_n^{(0)} = u_n \in L^2_{-\alpha,-\alpha}(I)$. Similarly

$$\begin{aligned}
\int_0^T (u_n^{(1)}(s))^2 (T-s)^{1-\alpha} s^{1-\alpha} ds &= \int_0^{\varepsilon_1} ((u_n^{(1)}(s))^2 (T-s)^{1-\alpha} s^{1-\alpha} ds + \int_{\varepsilon_1}^T ((u_n^{(1)}(s))^2 (T-s)^{1-\alpha} s^{1-\alpha} ds \\
&< K_1^2 \int_0^{\varepsilon_1} s^{\alpha-1} (T-s)^{1-\alpha} s^{1-\alpha} ds + M_1^2 \int_{\varepsilon_1}^T (T-s)^{1-\alpha} s^{1-\alpha} ds \\
&= K_1^2 \frac{T^{2-\alpha} - (T-\varepsilon_1)^{2-\alpha}}{2-\alpha} + M_1^2 \left[\frac{2^{-3+2\alpha}\sqrt{\pi} T^{3-2\alpha}\Gamma(2-\alpha)}{\Gamma(\frac{5}{2}-\alpha)} \right. \\
&+ \left. \frac{\varepsilon_1(\varepsilon_1 T)^{1-\alpha} \,{}_2F_1(2-\alpha, -1+\alpha, 3-\alpha; \frac{\varepsilon_1}{T})}{-2+\alpha} \right] < \infty,
\end{aligned}$$

where ${}_2F_1(a,b,s;z)$ is the hyper-geometric function. Therefore $u_n^{(1)} \in L^2_{-\alpha+1,-\alpha+1}(I)$ and so $u_n \in B^1_{-\alpha,-\alpha}(I)$.

In fact, from [55], we know that $u_n^{(1)}(t) = Kt^{\alpha-1} + O(t^{2\alpha-1})$. This means $u_n^{(2)}(t) = O(t^{\alpha-2})$, i.e. there are positive constants ε_2, K_2 such that $|u_n^{(2)}(t)| < K_2 t^{\alpha-2}$, $\forall 0 < t < \varepsilon_2$. Differentiating once and twice both sides of equation (19) with respect to t yields the expressions

$$\begin{aligned}
D^{1+\alpha}u_n &= O(t^{\alpha-1}), \\
D^{2+\alpha}u_n &= O(t^{\alpha-2}).
\end{aligned}$$

Again, there are positive constants $\varepsilon_{1+\alpha}, K_{1+\alpha}, \varepsilon_{2+\alpha}, K_{2+\alpha}$ such that $|D^{1+\alpha}u_n(t)| < K_{1+\alpha} t^{\alpha-1}$, $\forall 0 < t < \varepsilon_{1+\alpha}$ and $|D^{2+\alpha}u_n(t)| < K_{2+\alpha} t^{\alpha-2}$, $\forall 0 < t < \varepsilon_{2+\alpha}$.

Moreover, since u_n belongs to $C[0,T]$, so does $D^{\alpha}u_n$. Now, the first and second derivatives of u_n belong to $C(0,T]$, so do $D^{1+\alpha}u_n$ and $D^{2+\alpha}u_n$. Denote

$$M_{\alpha} := \sup_{0\le t\le T} D^{\alpha}u_n(t), \quad M_{1+\alpha} := \sup_{\varepsilon_{1+\alpha}\le t\le T} D^{1+\alpha}u_n(t), \quad M_{2+\alpha} := \sup_{\varepsilon_{2+\alpha}\le t\le T} D^{2+\alpha}u_n(t).$$

We have:

$$\int_0^T (D^{\alpha}u_n(s))^2\,ds < M_{\alpha}^2 T < \infty,$$

and so $D^{\alpha}u_n \in L^2_{0,0} = L^2$. Moreover,

$$\begin{aligned}\int_0^T \left(D^{1+\alpha}u_n(s)\right)^2 (T-s)s\,ds &= \int_0^{\varepsilon_{1+\alpha}} \left(D^{1+\alpha}u_n(s)\right)^2 (T-s)s\,ds + \int_{\varepsilon_{1+\alpha}}^T \left(D^{1+\alpha}u_n(s)\right)^2 (T-s)s\,ds \\ &< K_{1+\alpha}^2 \frac{\varepsilon_{1+\alpha}^{2\alpha}(T+2\varepsilon_{1+\alpha}(T-\varepsilon_{1+\alpha}))}{2\alpha(1+2\alpha)} + M_{1+\alpha}^2\left(\frac{T^3-T\varepsilon_{1+\alpha}^2}{2} - \frac{T^3-\varepsilon_{1+\alpha}^3}{3}\right) < \infty,\end{aligned}$$

and so $D^{1+\alpha}u_n \in L^2_{1,1}$. Also we have

$$\begin{aligned}\int_0^T \left(D^{2+\alpha}u_n(s)\right)^2 (T-s)^2 s^2\,ds &= \int_0^{\varepsilon_{2+\alpha}} \left(D^{2+\alpha}u_n(s)\right)^2 (T-s)^2 s^2\,ds \\ &+ \int_{\varepsilon_{2+\alpha}}^T \left(D^{2+\alpha}u_n(s)\right)^2 (T-s)^2 s^2\,ds \\ &< K_{2+\alpha}^2\varepsilon_{2+\alpha}^{2\alpha}\left[\frac{\varepsilon_{2+\alpha}}{1+2\alpha} - T\left(\frac{1}{\alpha} + \frac{T}{\varepsilon_{2+\alpha}-2\alpha\varepsilon_{2+\alpha}}\right)\right] \\ &+ M_{2+\alpha}^2\left[-\frac{\varepsilon_{2+\alpha}^5}{5} + \frac{T\varepsilon_{2+\alpha}^4}{2} - \frac{T^2\varepsilon_{2+\alpha}^3}{3} + \frac{T^5}{30}\right] < \infty,\end{aligned}$$

and so $D^{2+\alpha}u_n \in L^2_{2,2}$. So $u_n \in \mathcal{B}^2_{-\alpha,-\alpha}$, and the desired result follows.

Following the same reasoning as above for the integral representation of equation (18), it is straightforward to see that the solution, u, of the fractional Riccati equation (18) with zero initial condition belongs to $C(I)\cap B^1_{-\alpha,-\alpha}(I)\cap\mathcal{B}^2_{-\alpha,-\alpha}(I)$. In particular, $u\in L^2_{-\alpha,-\alpha}(I)$ and $D^{\alpha+2}u \in L^2_{2,2}$. $\square$

It is worth noting in the passing that based on Theorem 2, the smoother the solution of a fractional differential equation is, the higher the rate of convergence of the spectral collocation approximation which will be obtained.

Theorem 4. Starting from the initial starting point introduced in Remark 5, the convergence rate of the proposed quasi-linearization spectral collocation method to solve the fractional Riccati equation (18) is given by:

$$\|u-\widehat{u}_{n,N}\|_{\infty} \le C_1 2^{-n}\theta^{2^n} + C_2 N^{-1}\left\|D^{\alpha+2}u_n\right\|_{L^2_{2,2}}, \tag{28}$$

in which C_1 and C_2 are some constants independent of n and N and

$$\theta = \frac{8c_2\Gamma(1+\alpha)T^{\alpha}\eta}{[\Gamma(1+\alpha)-MT^{\alpha}]^2} < 1,$$

for M and η as defined in Remark 5.

Proof. In order to establish the required result, we use the triangle inequality to write

$$\|u-\widehat{u}_{n,N}\|_\infty \le \|u-u_n\|_\infty + \|u_n-\widehat{u}_{n,N}\|_\infty,$$

which by using conclusions of Theorems 1, 2 and 3, could be re-written as

$$\|u-\widehat{u}_{n,N}\|_\infty \le C_1 2^{-n}\theta^{2^n} + C_2 N^{-1}\left\|D^{\alpha+2}u_n\right\|_{L^2_{2,2}},$$

which proves the relation (28). □

Although we know that the $L^2_{-\alpha,-\alpha}$ norm of $D^{\alpha+2}u_n$ is finite for all values of n, it is not easy to find an explicit bound in terms of n for this term. However, if we compute the global error in the $L^2_{-\alpha,-\alpha}$ norm (Theorem 5 in the remainder), we could find an explicit bound in terms of n and N.

The following Lemma provides some properties of Jacobi poly-fractonomials and the norms of weighted L^p spaces which will be used in the proof of Theorem 5.

Lemma 1. The following properties hold:

(i) $\left\|\widetilde{\mathcal{P}}^\alpha_j\right\|^2_{L^2_{-\alpha,-\alpha}} = \left(\frac{2}{T}\right)^{2\alpha-1} C^{-\alpha,\alpha}_{j-1}$,

(ii) $\left\|\widetilde{\mathcal{P}}^\alpha_j\right\|_{L^1_{-\alpha,-\alpha}} \le \varpi^{1/2}\left\|\widetilde{\mathcal{P}}^\alpha_j\right\|_{L^2_{-\alpha,-\alpha}}$,

(iii) $\|u\|_{L^2_{-\alpha,-\alpha}} \le \varpi^{1/2}\|u\|_\infty$, for all $u\in L^2_{-\alpha,-\alpha}(I)$,

in which $\omega(t)=(T-t)^{-\alpha}t^{-\alpha}$ and $\varpi := \int_0^T \omega(t)dt = \frac{T^{1-2\alpha}\Gamma^2(1-\alpha)}{\Gamma(2-2\alpha)}$.

Proof. (i) Using the definition of Jacobi poly-fractonomials and $C^{-\alpha,\alpha}_{j-1}$, we have

$$\begin{aligned}
\left\|\widetilde{\mathcal{P}}^\alpha_j\right\|^2_{L^2_{-\alpha,-\alpha}} &= \left(\frac{2}{T}\right)^{2\alpha}\int_0^T \omega(t)\left(t^\alpha P^{-\alpha,\alpha}_{j-1}(x(t))\right)^2 dt\\
&= \left(\frac{2}{T}\right)^{2\alpha}\left(\frac{T}{2}\right)\int_{-1}^1 (1-x)^{-\alpha}(1+x)^{\alpha}\left(P^{-\alpha,\alpha}_{j-1}(x)\right)^2 dx\\
&= \left(\frac{2}{T}\right)^{2\alpha-1}\left\|P^{-\alpha,\alpha}_{j-1}\right\|^2_{L^2_{-\alpha,\alpha}} = \left(\frac{2}{T}\right)^{2\alpha-1} C^{-\alpha,\alpha}_{j-1}.
\end{aligned}$$

The expressions (ii) and (iii) are direct consequences of the Hölder inequality. □

Theorem 5. Starting from the initial starting point introduced in Remark 5, the convergence rate of the proposed quasi-linearization spectral collocation method to solve the fractional Riccati equation (18) is given by:

$$\|u-\widehat{u}_{n,N}\|_{L^2_{-\alpha,-\alpha}} \le C_3 2^{-n}\theta^{2^n}(N+1) + C_4 N^{-1}\left\|D^{\alpha+2}u\right\|_{L^2_{2,2}}, \tag{29}$$

in which C_3 and C_4 are some constants independent of n and N and θ is defined as in Theorem 4.

Proof. First, we note that

$$
\begin{aligned}
\|u-\widehat{u}_{n,N}\|_{L^2_{-\alpha,-\alpha}} &= \left\|\sum_{j=1}^{\infty}\xi_j\widetilde{\mathcal{P}}_j^{\alpha}-\sum_{j=1}^{N+1}\xi_{n,j}\widetilde{\mathcal{P}}_j^{\alpha}\right\|_{L^2_{-\alpha,-\alpha}}\\
&= \left\|\sum_{j=N+2}^{\infty}\xi_j\widetilde{\mathcal{P}}_j^{\alpha}+\sum_{j=1}^{N+1}(\xi-\xi_{n,j})\widetilde{\mathcal{P}}_j^{\alpha}\right\|_{L^2_{-\alpha,-\alpha}}\\
&\leq \|u-u_N\|_{L^2_{-\alpha,-\alpha}}+\sum_{j=1}^{N+1}|\xi_j-\xi_{n,j}|\left\|\widetilde{\mathcal{P}}_j^{\alpha}\right\|_{L^2_{-\alpha,-\alpha}}\\
&\leq \varpi^{1/2}\|u-u_N\|_{\infty}+\left(\frac{2}{T}\right)^{(2\alpha-1)/2}\sum_{j=1}^{N+1}|\xi_j-\xi_{n,j}|(C_{j-1}^{-\alpha,\alpha})^{1/2}\\
&\leq \varpi^{1/2}CN^{-1}\left\|D^{\alpha+2}u\right\|_{L^2_{2,2}}+\left(\frac{2}{T}\right)^{(2\alpha-1)/2}\sum_{j=1}^{N+1}|\xi_j-\xi_{n,j}|(C_{j-1}^{-\alpha,\alpha})^{1/2}, \qquad (30)
\end{aligned}
$$

where the last two lines are obtained using Lemma 1 and Theorem 2. Now, in order to bound the summation expression in the above inequality, note that for any $j\geq 1$, we have:

$$
\begin{aligned}
|\xi_j-\xi_{n,j}| &= \left|\left(\frac{T}{2}\right)^{2\alpha-1}\frac{1}{C_{j-1}^{-\alpha,\alpha}}\int_0^T(u(t)-u_n(t))\omega(t)\widetilde{\mathcal{P}}_j^{\alpha}(t)dt\right|\\
&\leq \left(\frac{T}{2}\right)^{2\alpha-1}\frac{1}{C_{j-1}^{-\alpha,\alpha}}\|u-u_n\|_{\infty}\left\|\widetilde{\mathcal{P}}_j^{\alpha}\right\|_{L^1_{-\alpha,-\alpha}}\\
&\leq \left(\frac{T}{2}\right)^{2\alpha-1}\frac{1}{C_{j-1}^{-\alpha,\alpha}}C_1 2^{-n}\theta^{2^n}\varpi^{1/2}\left\|\widetilde{\mathcal{P}}_j^{\alpha}\right\|_{L^2_{-\alpha,-\alpha}}\\
&\leq \left(\frac{T}{2}\right)^{2\alpha-1}\frac{1}{C_{j-1}^{-\alpha,\alpha}}C_1 2^{-n}\theta^{2^n}\varpi^{1/2}\left(\frac{2}{T}\right)^{(2\alpha-1)/2}(C_{j-1}^{-\alpha,\alpha})^{1/2}, \qquad (31)
\end{aligned}
$$

where the last two lines are obtained from Theorem 1 and Lemma 1, respectively. Putting inequalities (30) and (31) together, we get:

$$
\|u-\widehat{u}_{n,N}\|_{L^2_{-\alpha,-\alpha}}\leq\varpi^{1/2}CN^{-1}\left\|D^{\alpha+2}u\right\|_{L^2_{2,2}}+\varpi^{1/2}C_1 2^{-n}\theta^{2^n}(N+1),
$$

which completes the proof. □

It is worth nothing that although the second term of the error bound is increasing w.r.t N, the whole term tends to zero as both n and N go to infinity, since the rate of decay of $2^{-n}\theta^{2^n}$ is much faster than the growth rate of $N+1$. Although the constants C_3 and C_4 in (29) are hard to estimate, it gives still information on how the error is related to the two basic parameters n and N appearing in the two phases of the algorithm. In order to achieve accuracy as well as efficiency, we could make a balance between these two sources of error contribution which could be done in at least two different ways:

(i) determine n and N beforehand such that these two error terms are roughly of the same magnitude;

(ii) first fix N and then determine n such that the error is smaller than a given tolerance level.

We have pursued the second approach in this paper as will be made clear in the numerical experiments reported in the sequel.

Remark 6. The statement of Theorems 4 and 5 are also valid for more general families of nonlinear fractional Riccati differential equations with time-dependent coefficients of the form

$$D^{\alpha}u(t) = c_0(t) + c_1(t)u(t) + c_2(t)u^2(t),$$

in which $c_0(\cdot)$, $c_1(\cdot)$ and $c_2(\cdot)$ are twice continuously differentiable functions on $[0,T]$. These generalized FRODEs appear in modeling many different phenomena in fields such as physics, biology, physiology and optimal control [60, 5, 58, 1]. This indicates that the domain of application for the proposed method is far beyond the rough Heston model.

5.4. Numerical Experiments

In order to show the effectiveness of the above proposed methodology, we solve the Riccati equation (2)-(3) this time with the spectral collocation and Newton-Kantorovich linearization. We have implemented the algorithm on a laptop PC with a Intel(R) Core(TM) i5-2410M CPU at 2.30 GHz and 6 GB RAM using MATLAB R2017b programming environment. The results are shown in Table 2. Here, N_{fsc} is the number of collocation points and similar to Table 1, the rightmost column is calculated using the expression (10) with $\widehat{h}_{\text{Ad}}$ replaced with $\widehat{h}_{\text{fsc}}$ and $h(a,t_j)$ is the approximation of the solution with $N_{\text{fsc}} = 160$ collocation points. The reported times in the second last column of this table does not include the pre-allocation of the constants and calculation of poly-fractonomial basis functions. Also, the number of Newton iterations needed for convergence will be determined automatically within the algorithm which is reported in the third column of Table 2. Moreover, as illustrated in Figure 3, it properly approximates the solution for all values of a in combination with any other parameter sets and with any fixed number of basis functions without any explosion. Comparing the “time” and “MRE” columns of the two tables, we observe that the new method is very fast and at least quadratically convergent for small values of a and super-linearly convergent for larger values as illustrated in Figure 4 in which the reference line shows the linear rate of convergence.

It is worth mentioning that the numerical results are in accordance with Theorem 1 which analytically guarantees that the convergence of the algorithm is independent of the value of parameter a. In the sequel, we present the results of applying the above mentioned methodology in solving a practical financial engineering problem from SPX options markets.

6. Option Pricing and Calibration

In this section, we present some numerical experiments concerning the computational efficiency and complexity of the proposed method in pricing and calibration under the rough Heston model. For this purpose and in the pricing engine, we employ the Fourier option pricing technique of Lewis [47] and Carr and Madan [9].

6.1. Fourier Option Pricing Method

Having the characteristic function, $\Psi(a,T)$ in (1), we could employ the closed-form approximation to the pricing integral suggested by Lewis [46] (see also [47, 28]) which applies the inverse Fourier transform to provide an option valuation formula as a contour integral in the complex plane[5]. Based on this formula, the call option price could be calculated using the expression:

$$C(S,K,T) = Se^{-qT} - \frac{1}{\pi}\sqrt{SK}e^{-(r+q)T/2}\int_0^{\infty}\frac{\Re[e^{iak}\Psi(a-i/2,T)]}{a^2+\frac{1}{4}}da, \tag{32}$$

[5]It should be noted that a similar approach to Lewis [46] is described by Lipton [52] in the context of FX option pricing. The Lewis-Lipton approach generalizes the method of Carr and Madan [9] since their dampening factor corresponds to the path of the contour integral in the Fourier transform.

Table 2: Approximate solution of the fractional Riccati equation at $T = 2$ and different values of a, and $\alpha = 0.6$, $\rho = -0.5$, $\lambda = 0.2$, $\nu = 0.5$ using Jacobi poly-fractonomials and Newton iteration. N_{fsc} is the number of Jacobi poly-fractonomials used for the interpolation. The Newton iteration stops when $\max(\Re(\|u_n - u_{n-1}\|)) < 10^{-8}$ and n is the number of Newton iterations to achieve this precision.

a	N_{fsc}	n	$\Re[\widehat{h}_{\text{fsc}}(a,T)]$	$\Im[\widehat{h}_{\text{fsc}}(a,T)]$	time (s)	MRE(N_{fsc})
10	5	4	-49.0807046952	14.8375090685	0.003	0.0031
	10	4	-49.0787853972	14.8407277479	0.004	7.6e-04
	20	4	-49.0785452921	14.8408126238	0.005	1.8e-04
	40	4	-49.0785130448	14.8408280659	0.006	4.0e-05
	80	4	-49.0785091334	14.8408301719	0.01	7.3e-06
	160	4	-49.0785086836	14.8408304252	0.03	—
100	5	7	-8.04384294e+02	4.62076565e+02	0.006	0.0564
	10	6	-8.17306929e+02	4.63830399e+02	0.006	0.0154
	20	6	-8.16607059e+02	4.64224853e+02	0.007	0.0028
	40	6	-8.16609239e+02	4.64226616e+02	0.008	4.1e-04
	80	6	-8.16608991e+02	4.64226076e+02	0.01	7.0e-05
	160	6	-8.16608982e+02	4.64226055e+02	0.04	—
1000	5	8	-7.64716391e+03	4.41402125e+03	0.002	0.2485
	10	8	-9.06210022e+03	5.21767134e+03	0.005	0.1158
	20	7	-8.75517161e+03	5.03733388e+03	0.007	0.0459
	40	7	-8.63261762e+03	4.97061137e+03	0.009	0.0130
	80	7	-8.61126258e+03	4.96493275e+03	0.01	0.0024
	160	7	-8.61053341e+03	4.96539753e+03	0.02	—
1500	5	9	-1.13712037e+04	6.56299912e+03	0.001	0.2881
	10	8	-1.37467576e+04	7.92408707e+03	0.002	0.1378
	20	8	-1.32561485e+04	7.63630767e+03	0.005	0.0593
	40	7	-1.30133620e+04	7.49537785e+03	0.007	0.0200
	80	7	-1.29465085e+04	7.46498434e+03	0.03	0.0044
	160	7	-1.29406868e+04	7.46536011e+03	0.08	—

in which $k = \log(S/K) + (r - q)T$, and q is the dividend rate.

6.1.1. *Pricing Experiment*

In order to compare the pricing performance of the proposed method with the two available competitors in the literature (the fast Hybrid scheme of Callegaro et al. [32] and the fractional Adams method of El Euch and Rosenbaum [20]), we have prepared Table 3 based on the data presented in [32] for the other two methods. The details of parameter choices for the other two schemes is presented in [32] with enough detail but we only stress here that the step-size of the fractional Adams method is chosen such that the obtained results coincide (up to a tolerance level of 10^{-2}) with the ones obtained from the fast hybrid scheme in term of the implied volatilities. A range of maturities from 1 day to 2 years and a wide spectrum of moneyness[6] values is used in the comparison. The choice of N in FSC depends naturally on T (as shown in (28)) but we

[6]The moneyness of an option is equal to the ratio between the strike price and the current price of the underlying asset.

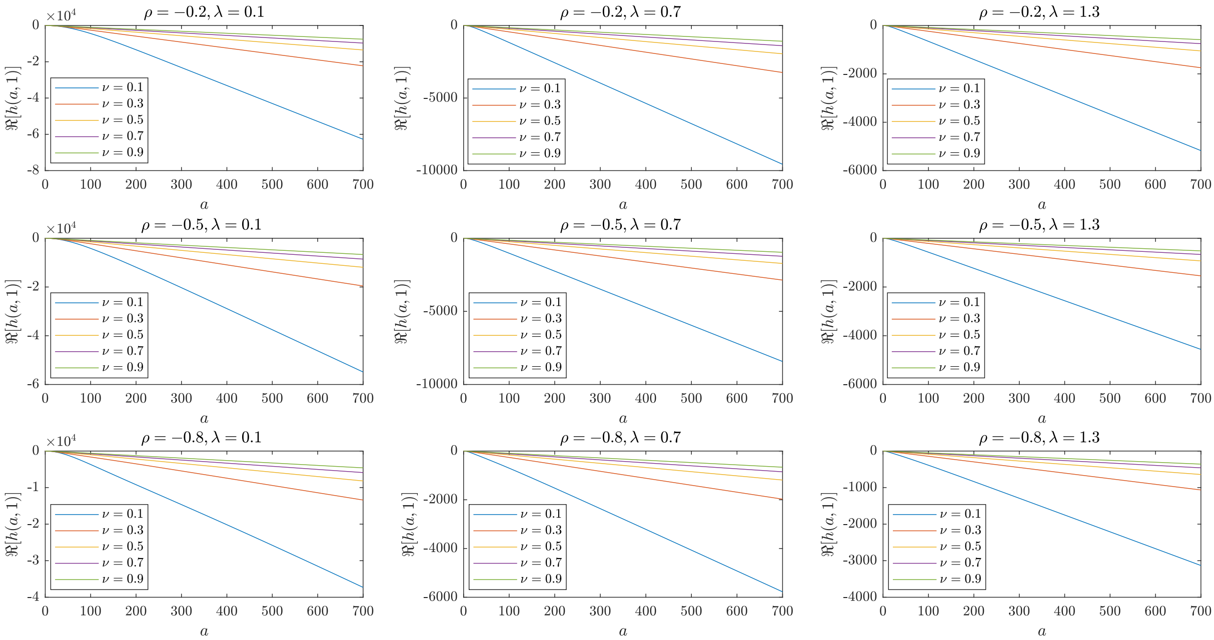

Figure 3: The fractional spectral collocation method successfully generates the result for all values of a.

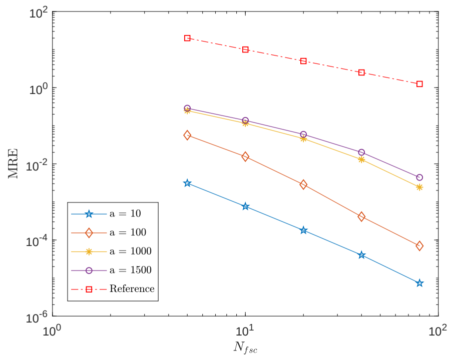

Figure 4: Rate of convergence for fractional spectral collocation method.

have not tried at all to do this choice optimally as it has a slight influence on the reported times and prices. The times reported in Table 3 for the FSC method are inclusive of all the computations and pre-allocations.

Unless for the case of 1 day maturity ($T = 1/256$) and the strikes greater than 100%, the accuracy of the FSC and Hybrid schemes are comparable but the time efficiency of the FSC is better than the other schemes. For 1 day maturity and larger than 100% strikes, it seems that the FSC scheme has resulted in smaller prices for the call option which needs more careful investigation and analysis to identify causes and sources of this particular behavior.

Table 3: Call option prices obtained by three methods: FSC (the quasi-linearized fractional spectral collocation), Hybrid (the fast hybrid scheme of [32]) and Adams (the fractional Adams methods used in [20]). The parameters are as in [20] ($\alpha = 0.62, \lambda = 0.1, \rho = -0.681, \nu = 0.331, V_0 = 0.0392$ and $\theta = 0.3156$.). Maturities range from 1 day till 2 years while strikes vary in the range between 80% – 120% of the moneyness. The computational time (CT) is in milliseconds (i.e. 10^{-3}s). The number of series terms retained in Hybrid scheme is set to 128. We choose the number of series terms in FSC equal to $N = 5$ for 1 day, $N = 10$ for 1 week, $N = 15$ for 1 month, $N = 20$ for 6 months, $N = 25$ for 1 year and $N = 30$ for two years of maturities.

		1 day	1 week	1 month	6 month	1 year	2 year
Strike		Price(CT)	Price(CT)	Price(CT)	Price(CT)	Price(CT)	Price(CT)
80%	FSC	20(42)	20(46)	20.0005(58)	20.6110(61)	22.1360(63)	25.4284(65)
	Hybrid	20(180)	20(154)	20.0005(410)	20.6112(672)	22.1366(553)	25.4301(667)
	Adams	19.9988(108)	20(108)	20.0005(108)	20.6095(16095)	22.1331(37768)	25.4258(244381)
85%	FSC	15(39)	15(41)	15.0108(48)	16.2804(62)	18.3525(99)	22.2082(113)
	Hybrid	15(170)	15(164)	15.0108(421)	16.2807(689)	18.3529(553)	22.2091(596)
	Adams	15(107)	15(108)	15.0108(9282)	16.2783(16658)	18.3486(39557)	22.2044(244056)
90%	FSC	10(36)	10.0002(40)	10.1143(53)	12.3943(63)	14.9668(102)	19.2888(112)
	Hybrid	10(155)	10.0002(155)	10.1144(423)	12.3948(671)	14.9672(549)	19.2898(594)
	Adams	9.9985(109)	10.0002(109)	10.1141(9598)	12.3924(38252)	14.9623(38236)	19.2847(248059)
95%	FSC	5(42)	5.0491(29)	5.6722(46)	9.0631(81)	12.0053(110)	16.6665(112)
	Hybrid	5.0003(156)	5.0491(156)	5.6723(410)	9.0636(676)	12.0059(557)	16.6676(594)
	Adams	4.9967(112)	5.0489(2178)	5.6712(2359)	9.0609(37826)	12.0006(38672)	16.6622(248779)
100%	FSC	0.5011(25)	1.1346(32)	2.3895(46)	6.3492(61)	9.4732(113)	14.3308(116)
	Hybrid	0.5012(154)	1.1347(156)	2.3896(416)	6.3497(672)	9.4737(548)	14.3319(596)
	Adams	0.5071(108)	1.1339(108)	2.3885(112)	6.3461(16076)	9.4683(38909)	14.3264(249641)
105%	FSC	3.38e-06(35)	0.0411(34)	0.6808(46)	4.2545(61)	7.3558(108)	12.2665(113)
	Hybrid	6.39e-05(159)	0.04113(125)	0.6809(416)	4.2550(666)	7.3563(551)	12.2676(601)
	Adams	6.33e-04(121)	0.04118(108)	0.6804(2141)	4.2516(16539)	7.3510(38256)	12.2621(258262)
110%	FSC	9.49e-11(31)	9.26e-05(40)	0.1205(46)	2.7247(63)	5.6227(85)	10.4551(112)
	Hybrid	2.37e-05(163)	9.22e-05(125)	0.1205(414)	2.7251(681)	5.6234(562)	10.4562(599)
	Adams	2.06e-03(109)	9.28e-05(71309)	0.01205(2259)	2.7223(16670)	5.6195(73084)	10.4508(248696)
115%	FSC	2.86e-08(35)	1.04e-09(54)	0.0125(48)	1.6676(62)	4.2337(86)	8.8762(113)
	Hybrid	1.51e-05(155)	6.82e-09(155)	0.0124(410)	1.6680(683)	4.2343(582)	8.8773(593)
	Adams	1.49e-03(107)	8.85e-07(70685)	0.0125(2194)	1.6658(16302)	4.2307(73086)	8.8720(248391)
120%	FSC	2.69e-08(40)	1.56e-13(46)	7.33e-04(54)	0.9759(62)	3.1419(86)	7.5083(120)
	Hybrid	1.14e-05(196)	1.80e-13(156)	7.32e-04(414)	0.9761(667)	3.1424(577)	7.5093(593)
	Adams	1.08e-03(110)	3.70e-7(108)	7.37e-04(2316)	0.9674(16269)	3.1393(73184)	7.5042(245999)

Table 4: number of available option contracts corresponding to different strike prices considered in the calibration experiment for each maturity (in years).

T	0.1178	0.2329	0.6164	1.3644
M_T	57	5	7	3

6.2. Calibration Experiment

Equipped with a pricing algorithm, we try to calibrate the parameters of the model using a suitable error criterion in terms of the model parameters. The calibration algorithm finds the parameters of the model for a set of market data by minimizing the sum of squared differences between the market implied volatility (IV) and those generated from the model.

The option prices on SPX (S&P 500 index) are extracted from Chicago Board Options Exchange's database (see www.cboe.com), on Feb 02 2017 at 13:39 ET. Only the options with positive volume are considered in the calibration. The risk-free rate of return is set to be 0.02 and for each maturity, the dividend yield is calculated from the Put-Call parity formula:

$$P(S,t) = C(S,t) - S\exp(-q(T-t)) + K\exp(-r(T-t)).$$

From the six parameters of the model for each maturity T, two of them (θ and α) are fixed to the values $\alpha = 0.6$ and $\theta = 0.1$ by trial and error. We must note that if we don't prefix the parameter α during the calibration process, the time efficiency of the calibration procedure may be degraded slightly but the algorithm still performs well, without any explosion. The other four parameters ($[\rho, \nu, V_0, \lambda] =: \Theta$) are now calibrated by solving the following optimization problem:

$$\begin{aligned}
&\min_{\Theta} \sum_{i=1}^{M_T} |V^{\Theta}_{T,i} - V^{*}_{T,i}|^2,\\
&\text{s.t.} -\frac{1}{\sqrt{2}} < \rho < 0,\\
&\qquad \nu,\ V_0,\ \lambda > 0,
\end{aligned}$$

in which M_T is the number of options with different strikes considered in our calibration experiment (see Table 4), $V^{\Theta}_T = [V^{\Theta}_{T,1}, V^{\Theta}_{T,2}, \cdots, V^{\Theta}_{T,M_T}]$ is the vector of implied volatilities corresponding to option prices obtained from rough Heston model for the parameter set Θ and $V^{*}_T = [V^{*}_{T,1}, V^{*}_{T,2}, \cdots, V^{*}_{T,M_T}]$ is the vector of market implied volatilities for maturity T. For each Maturity, the AARE and MARE columns in Tables 5 and 6 are the average and the maximum value of the relative error, across all strikes, defined respectively by

$$\begin{aligned}
\text{AARE}(T,\Theta) &= \frac{1}{M_T} \sum_{i=1}^{M_T} \frac{|V^{\Theta}_{T,i} - V^{*}_{T,i}|}{V^{*}_{T,i}},\\
\text{MARE}(T,\Theta) &= \max_{i=1\cdots M_T} \frac{|V^{\Theta}_{T,i} - V^{*}_{T,i}|}{V^{*}_{T,i}}.
\end{aligned}$$

Although the errors of the two methods does not indicate a notable difference, applying the fractional Adams method will cause some technical difficulties in the calibration process: to obtain the call price, the integral term appearing in the right-hand side of (32) should be truncated into a finite interval. For each maturity, the upper limit of this finite interval should be adjusted beforehand, otherwise the Adams method will explode for large values of a. Many trial and error experiments are conducted to achieve suitable

Table 5: Calibrated parameters $\Theta = [\rho, \nu, V_0, \lambda]$ using the combined quasi-linearization and spectral collocation. Parameters $\alpha = 0.6$ and $\theta = 0.1$ are prefixed. The initial guess for the optimization procedure is $\rho_0 = -0.5, \nu_0 = 0.5, V_0 = \text{mean}(V_T^*)$ and $\lambda_0 = 0.4$.

T	N_{fsc}	ρ	ν	V_0	λ	AARE	MARE	CPU time (s)
0.1178	5	-0.6406	0.6687	0.0063	0.5972	0.0183	0.0503	251.0477
	10	-0.6362	0.4609	1.0e-06	0.9670	0.0186	0.0512	313.2552
	20	-0.6361	0.4631	1.0e-06	0.9644	0.0186	0.0513	469.4882
	40	-0.6361	0.4637	1.0e-06	0.9637	0.0186	0.0513	1760.1473
	64	-0.6361	0.4638	1.0e-06	0.9635	0.0186	0.0513	4098.1155
0.2329	5	-0.7264	0.6811	0.0069	0.6050	0.0051	0.0095	12.3341
	10	-0.7222	0.6762	0.0067	0.5975	0.0052	0.0098	14.6119
	20	-0.7206	0.6742	0.0066	0.5944	0.0053	0.0099	27.2793
	40	-0.7201	0.6736	0.0066	0.5935	0.0053	0.0100	75.4406
	64	-0.7200	0.6734	0.0066	0.5933	0.0053	0.0100	205.5123
0.6164	5	-0.7855	0.6685	0.0049	0.6519	0.0013	0.0022	11.9977
	10	-0.7825	0.6698	0.0046	0.6517	0.0016	0.0026	15.3662
	20	-0.7816	0.6740	0.0046	0.6470	0.0017	0.0028	29.8595
	40	-0.7813	0.6736	0.0046	0.6481	0.0017	0.0028	87.4910
	64	-0.7812	0.6733	0.0045	0.6488	0.0017	0.0028	240.4867
1.3644	5	-0.8061	0.7468	0.0045	0.7031	3.3e-07	3.9e-07	11.3848
	10	-0.8042	0.7438	0.0037	0.6997	1.0e-06	1.6e-06	13.7644
	20	-0.8036	0.7396	0.0032	0.7052	3.7e-07	5.1e-07	25.0779
	40	-0.8035	0.7416	0.0032	0.7031	5.3e-05	8.3e-05	64.2100
	64	-0.8035	0.7406	0.0032	0.7033	3.8e-07	4.8e-07	183.4643

Table 6: Calibrated parameters $\Theta = [\rho, \nu, V_0, \lambda]$ using the fractional Adams method. Parameters $\alpha = 0.6$, $\theta = 0.1$ are prefixed. The initial guess for the optimization procedure is $\rho_0 = -0.5,\ \nu_0 = 0.5, V_0 = \text{mean}(V_T^*)$ and $\lambda_0 = 0.4$ for all T except for $T = 0.6164$ for which we have used $\rho_0 = -0.8$.

T	$a_{\max}$	N_a	N_t	ρ	ν	V_0	λ	AARE	MARE	CPU time (s)
0.1178	100	512	256	-0.6387	0.4537	1.0e-06	0.9827	0.0166	0.0538	882.1240
0.2329	80	256	80	-0.7182	0.6955	0.0072	0.6161	0.0015	0.0025	34.4670
0.6164	60	256	80	-0.7831	0.6925	0.0057	0.6533	0.0011	0.0021	30.3321
1.3644	30	256	80	-0.7997	0.7639	0.0037	0.7586	1.3e-06	3.0e-06	55.4553

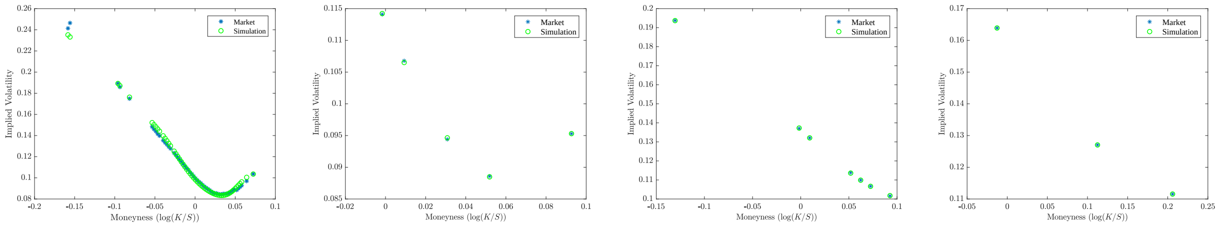

(a) $T = 0.1178$ (b) $T = 0.2329$ (c) $T = 0.6164$ (d) $T = 1.3644$

Figure 5: Market and calibrated implied volatilities for different maturities using the fractional Adams method.

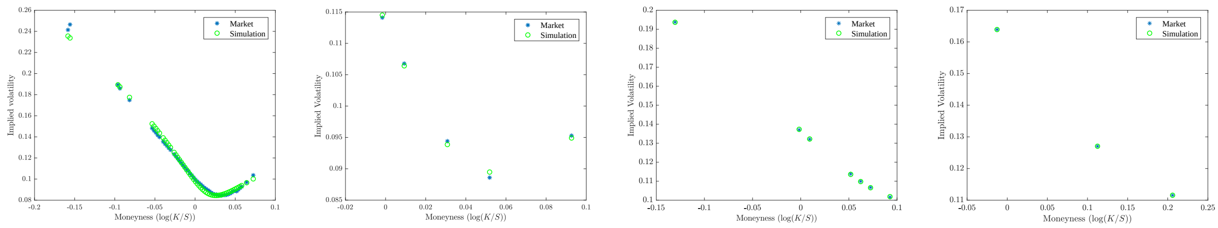

(a) $T = 0.1178$ (b) $T = 0.2329$ (c) $T = 0.6164$ (d) $T = 1.3644$

Figure 6: Market and calibrated implied volatilities for different maturities using the combined quasilinearization and spectral collocation method.

values of $a_{\max}$, N_a and N_t for different maturities, see Table 6. In contrast, the combined quasilinearization - spectral collocation method works properly well for all values of a which allows working with the integral without any formal truncation, using the "quadgk" function in the MATLAB programming environment.

It must be noted also that we don't need to use more than 5 collocation points, as it is not rewarding in terms of the performance (error) of the calibration procedure. In addition, the Adams method is time-consuming, since a "for" loop on the time grid is inevitable. As the numerical experiment shows, the proposed fractional spectral method reduces the CPU time at least to one third of the Adams method. This reduction will be significant for large data sets, as we see for $T = 0.1178$ where 57 options data are processed. It is worth noting that the fractional Adams method uses a partition consisting of only 512 or 256 values of a in the integration procedure, while "quadgk" uses a partition of much bigger size. Moreover, collocation method seems to be independent of the number of poly-fractonomial basis, i.e. increasing the degree of Jacobi polynomials doesn't improve the error and only five basis functions are enough to gain the same or better precision as that of the fractional Adams method.

Finally, in order to show that the calibration procedure is robust with respect to the number of option contracts in the sample, we repeat the calculations corresponding to the maturity $T = 0.1178$ now with the aid of a sub-sample including 9 contracts selected evenly from the main sample. The results are reported in Table 7. They clearly demonstrate that the AARE and MARE error indicators are normalized deviation measures between the market-implied and model-implied volatilities.

7. Conclusion

In this paper, we have presented an efficient scheme based on quasi-linearization followed by spectral collocation using Jacobi poly-fractonomials to solve fractional Riccati differential equations. We provide

Table 7: Calibrated parameters $\Theta = [\rho, \nu, V_0, \lambda]$ using the combined quasi-linearization and spectral collocation. Parameters $\alpha = 0.6$ and $\theta = 0.1$ are prefixed. The initial guess for the optimization procedure is $\rho_0 = -0.5, \nu_0 = 0.5, V_0 = \text{mean}(V_T^*)$ and $\lambda_0 = 0.4$. The options data include a subsample of 9 contracts from the original 57 contracts.

T	N_{fsc}	ρ	ν	V_0	λ	AARE	MARE	CPU time (s)
0.1178	5	-0.6309	0.7539	0.0073	0.5601	0.0205	0.0315	47.3779
	10	-0.6263	0.4844	1.0e-06	0.9902	0.0208	0.0332	56.9425
	20	-0.6262	0.4867	1.0e-06	0.9876	0.0208	0.0333	99.0243
	40	-0.6262	0.4873	1.0e-06	0.9868	0.0208	0.0333	251.8572
	64	-0.6262	0.4875	1.0e-06	0.9866	0.0208	0.0333	793.4031

sufficient conditions under which the method is convergent and also obtain its convergence rate. We show the applicability of the method in pricing and calibration under rough Heston model recently introduced into the field of finance. We propose the new scheme as a reliable alternative to the fractional Adams method previously proposed to solve the problem. Comparisons with a hybrid scheme based on fractional power series expansions also shows the effectiveness of the proposed methodology. Among the possible ways to improve the method, it is possible to study the effect of adaptive selection of collocation nodes on the efficiency and stability of the method.

Acknowledgments

The first author gratefully acknowledges scholarship from the Ministry of Science, Research and Technology (Iran) and the Eiffel Excellence scholarship (France) which financially supported her visit to University Paris 7 (LPMA - Laboratoire de Probabilits et Modles Alatoires) during which this research was born. The authors would like to sincerely thank Professors Peter Tankov and Kathrin Glau for providing valuable and helpful suggestions and comments on the construction of the research question and the progress of the paper. The second author also gratefully acknowledges support by the Institute for Advanced Studies in Basic Sciences (IASBS) Research Council under grant No. G2017IASBS22614.

Appendix A. On Weak Singularity of Solutions to the Volterra Integral Equation (8)

Using the results of Miller and Feldstein [55] on the regularity of solutions to Volterra integral equations, we show that $h(a,t)$ is weakly singular of order one, in the sense that

$$\frac{d}{dt}h(a,t) = (a^2 - a)\frac{\alpha}{2(1+\alpha)}t^{\alpha-1} + O(t^{2\alpha-1}). \tag{33}$$

Definition 1 ([55], Definition 1)**.** Suppose that ν is a nonnegative integer and f is a function defined on $(0,T]$ (or $[0,T]$). Then f is said to be weakly singular of order ν, if and only if

- $f \in C(0,T]$ if $\nu = 0$ or $f \in C^{\nu-1}[0,T] \cap C^{\nu}(0,T]$ if $\nu > 0$;
- for each $\varepsilon > 0$, the function $f^{(\nu)}(t)$ is absolutely continuous on the interval $\varepsilon \leq t \leq T$; and

- the function α_ν defined by

$$\alpha_\nu(t,f) = f(T) + \int_t^T |f^{(\nu+1)}(s)|ds, \quad 0 < t \leq T,$$

is of class $L^1(0,T)$.

Theorem 6 ([55], Section 5)**.** Suppose that $x(t)$ is the solution of

$$x(t) = f(t) + \int_0^t (t-s)^{(\nu-p)} g(s,x(s))ds, \quad 0 \leq t \leq T,$$

where $\nu \geq 0$ is an integer and $0 < p < 1$. If f and g are sufficiently smooth, then $x(\cdot)$ is weakly singular of order $\nu+1$ and $x^{(\nu+1)}(t) = O(t^{-p})$ as $t \to 0$. Moreover,

$$\frac{d^{(\nu+1)}x(t)}{dt^{(\nu+1)}} = f^{(\nu+1)}(0) + Kt^{-p} + O(t^{1-p}), \quad \nu \geq 1,$$

in which $K = 2g(0, f(0))(\nu+1-p)\cdots(1-p)/(\nu+2-p)$.

Using this theorem and setting $\nu = 0$, we get

$$\frac{dx(t)}{dt} = Kt^{-p} + O(t^{1-2p}),$$

and so the relation (33) will be obtained easily.

Appendix B. A General Stability Result for the Fractional Adams Method

Let h be a fixed step-size and $t_j, j = 0,1,\cdots,n$ and $w_{n,j}, j = 0,1,\cdots,n$ be the nodes and weights of a given quadrature rule for discretizing integrals. Stability analysis for a numerical scheme of the form

$$y_n = g_n + h\sum_{j=0}^{n} w_{n,j} K(t_n,t_j,y_j), \quad n = p+1,\cdots,N_h, \tag{34}$$

for a Volterra integral equation

$$x(t) = f(t) + \int_0^t K(t,s,x(s))ds, \quad 0 \leq t \leq T.$$

could be conducted in several different veins. The most natural approach (called here the "perturbation stability analysis") is concerned with analyzing whether or not a small perturbation in the initial values $(y_0, y_1, \cdots, y_{p-1})$ and/or the right-hand side terms, $g(t_n), n = 0,1,\cdots,N_h$ will cause a large error in the numerical solution. More precisely we have the following.

Definition 2. Let the perturbations Δy_j, $j = 0,\cdots,p$ and Δg_n, $n = 0,1,\cdots,N_h$ be admissible in the sense that

$$\Delta := \sup_{j=0,1,\cdots,p} \Delta y_j + \sup_{n=0,1,\cdots,N_h} \Delta g_n < \infty.$$

Let also the values $y_n + \Delta y_n$, $n = p+1,\cdots,N_h$ satisfy the *perturbed problem*

$$y_n + \Delta y_n = g_n + \Delta g_n + \sum_{j=0}^{n} w_{n,j} K(t_n,t_j,y_j+\Delta y_j).$$

Then the solution, y_n of (34) is conditionally stable with respect to perturbations $\Delta y_j,\ j = 0,\cdots,p$ and $\Delta g_n, n = 0,1,\cdots,N_h$, if and only if

$$\sup_{n=p+1,\cdots,N_h} |\Delta y_n| < C\Delta,$$

for some constant $C > 0$.

Based on Theorem 3.3 in [49], the fractional Adams method is conditionally stable in the sense of Definition 2.

Appendix C. A Brief Outline of the Fast Hybrid Scheme of Callegaro et al. [32]

In [32], the authors propose a novel hybrid scheme based on fractional power series expansion accompanied with time discretization for solving (2)-(3). The main idea is to use an expansion of the form

$$h(t) = h_{\lambda,\rho,\nu}(t) = \sum_{k\geq 0} a_k t^{k\alpha} \tag{35}$$

and then applying the D^{α} operator to this series expansion and inserting it into the equation. Doing so they obtain a recursive relation on the coefficients of the form

$$a_0 = 0, \quad a_1 = \frac{\nu}{\Gamma(\alpha+1)}, \quad a_{k+1} = (\lambda a_k^{*2} + \mu a_k)\frac{\Gamma(\alpha k+1)}{\Gamma(\alpha k+\alpha+1)}, \quad k \geq 1,$$

in which a_k^{*2} denotes the discrete convolution defined by

$$a_k^{*2} = \sum_{l=0}^{k} a_l a_{k-l}, \quad k \geq 0,$$

They show that the convergence radius, R_h of the fractional power series (35) is bounded as

$$0 < R_{\text{lower}} < R_h < R_{\text{upper}},$$

and the series is absolutely convergent for every $t \in [0, R_h)$. In order to control the error induced by truncating the series expansion (35) at any order n_0, they derive some computable errors bounds and then propose a mixed (hybrid) scheme by merging two methods, one based on (35) for approximating h and the other based on time discretization to approximate $I^1(h)(t)$ and $I^{1-\alpha}(h)(t)$. In the time discretization phase, they use the Richardson-Romberg extrapolation based on a conjecture on the existence of an expansion of the time discretization error.

References

[1] Brian D. O. Anderson and John B Moore. *Optimal Control: Linear Quadratic Methods*. Courier Corporation, 2007.

[2] Ioannis K Argyros. *Convergence and applications of Newton-type iterations*. Springer Science & Business Media, 2008.

[3] Richard T Baillie. Long memory processes and fractional integration in econometrics. *Journal of Econometrics*, 73(1):5–59, 1996.

[4] Dumitru Baleanu, Kai Diethelm, Enrico Scalas, and Juan J. Trujillo. *Fractional Calculus: Models and Numerical Methods*, volume 3. World Scientific, 2012.

[5] François Barthelat, Pablo Zavattieri, Chad S Korach, Barton C Prorok, and K Jane Grande-Allen. Mechanics of Biological Systems and Materials, volume 4: Proceedings of the 2013 Conference on Experimental and Applied Mechanics. 2014.

[6] Christian Bayer, Peter Friz, and Jim Gatheral. Pricing under rough volatility. *Quantitative Finance*, 16(6):887–904, 2016.

[7] Richard E Bellman and Robert E Kalaba. *Quasilinearization and Nonlinear Boundary-Value Problems*. Elsevier, 1965.

[8] Tomas Björk and Henrik Hult. A note on Wick products and the fractional Black–Scholes model. *Finance and Stochastics*, 9(2):197–209, 2005.

[9] Peter Carr and Dilip Madan. Option valuation using the fast Fourier transform. *Journal of Computational Finance*, 2(4):61–73, 1999.

[10] Fabienne Comte, Laure Coutin, and Éric Renault. Affine fractional stochastic volatility models. *Annals of Finance*, 8(2-3):337–378, 2012.

[11] Fabienne Comte and Eric Renault. Long memory in continuous-time stochastic volatility models. *Mathematical Finance*, 8(4):291–323, 1998.

[12] Nigel J Cutland, P Ekkehard Kopp, and Walter Willinger. Stock price returns and the Joseph effect: a fractional version of the Black–Scholes model. In *Seminar on Stochastic Analysis, Random Fields and Applications*, pages 327–351. Springer, 1995.

[13] Wesley Devauld. *Monte Carlo Methods for Derivative Pricing of Stochastic Volatility Models Driven by Fractional Brownian Motion*. PhD thesis, University of Calgary, 2013.

[14] Kai Diethelm. *The Analysis of Fractional Differential Equations: An Application-Oriented Exposition Using Differential Operators of Caputo Type*. Springer, 2010.

[15] Kai Diethelm, Neville J Ford, and Alan D Freed. A predictor-corrector approach for the numerical solution of fractional differential equations. *Nonlinear Dynamics*, 29(1):3–22, 2002.

[16] Kai Diethelm, Neville J Ford, and Alan D Freed. Detailed error analysis for a fractional adams method. *Numerical Algorithms*, 36(1):31–52, 2004.

[17] Beiping Duan, Zhoushun Zheng, and Wen Cao. Spectral approximation methods and error estimates for Caputo fractional derivative with applications to initial-value problems. *Journal of Computational Physics*, 319:108–128, 2016.

[18] Omar El Euch, Masaaki Fukasawa, and Mathieu Rosenbaum. The microstructural foundations of leverage effect and rough volatility. *Finance and Stochastics*, 22(2):241–280, 2018.

[19] Omar El Euch, Jim Gatheral, and Mathieu Rosenbaum. Roughening Heston. Unpublished results, 2018.

[20] Omar El Euch and Mathieu Rosenbaum. The characteristic function of rough Heston models. *Mathematical Finance*, 29(1):3–38, 2019.

[21] Martin Forde and Hongzhong Zhang. Asymptotics for rough stochastic volatility models. *SIAM Journal on Financial Mathematics*, 8(1):114–145, 2017.

[22] Bengt Fornberg. *A Practical Guide to Pseudospectral Methods*. Cambridge University Press, 1996.

[23] Jean-Pierre Fouque and Ruimeng Hu. Optimal portfolio under fast mean-reverting fractional stochastic environment. *SIAM Journal on Financial Mathematics*, 9(2):564–601, 2018.

[24] Jean-Pierre Fouque and Ruimeng Hu. Optimal portfolio under fractional stochastic environment. *Mathematical Finance*, 2018.

[25] Jean-Pierre Fouque, George Papanicolaou, and K Ronnie Sircar. *Derivatives in Financial Markets with Stochastic Volatility*. Cambridge University Press, 2000.

[26] Masaaki Fukasawa. Short-time at-the-money skew and rough fractional volatility. *Quantitative Finance*, 17(2):189–198, 2017.

[27] Josselin Garnier and Knut Sølna. Correction to Black–Scholes formula due to fractional stochastic volatility. *SIAM Journal on Financial Mathematics*, 8(1):560–588, 2017.

[28] Jim Gatheral. *The Volatility Surface: A Practitioner's Guide*, volume 357. John Wiley & Sons, 2011.

[29] Jim Gatheral, Thibault Jaisson, and Mathieu Rosenbaum. Volatility is rough. *Quantitative Finance*, 18(6):933–949, 2018.

[30] Jim Gatheral and Radoš Radoičić. Rational approximation of the rough Heston solution. *International Journal of Theoretical and Applied Finance*, 22(3):1950010, 2019.

[31] Stefan Gerhold, Christoph Gerstenecker, and Arpad Pinter. Moment explosions in the rough Heston model. *arXiv preprint arXiv:1801.09458*, 2018.

[32] Callegaro Giorgia, Grasselli Martino, and Pagès Gilles. Fast hybrid schemes for fractional riccati equations (rough is not so tough). *arXiv preprint arXiv:1805.12587*, 2018.

[33] Hamza Guennoun, Antoine Jacquier, Patrick Roome, and Fangwei Shi. Asymptotic behaviour of the fractional Heston model. *arXiv preprint arXiv:1411.7653*, 2014.

[34] Jan S Hesthaven, Sigal Gottlieb, and David Gottlieb. *Spectral Methods for Time-Dependent Problems*, volume 21. Cambridge University Press, 2007.

[35] Steven L Heston. A closed-form solution for options with stochastic volatility with applications to bond and currency options. *The Review of Financial Studies*, 6(2):327–343, 1993.

[36] Blanka Horvath, Antoine Jacquier, and Peter Tankov. Volatility options in rough volatility models. *arXiv preprint arXiv:1802.01641*, 2018.

[37] M Yousuff Hussaini, David A Kopriva, and Anthony T Patera. Spectral collocation methods. *Applied Numerical Mathematics*,

5(3):177–208, 1989.
[38] Eduardo Abi Jaber, Martin Larsson, and Sergio Pulido. Affine Volterra processes. *arXiv preprint arXiv:1708.08796*, 2017.
[39] Antoine Jacquier, Claude Martini, and Aitor Muguruza. On VIX futures in the rough Bergomi model. *Quantitative Finance*, 18(1):45–61, 2018.
[40] Antoine Jack Jacquier and Mugad Oumgari. Deep ppdes for rough local stochastic volatility. *Available at SSRN 3400035*, 2019.
[41] Hossein Jafari, Haleh Tajadodi, and Dumitru Baleanu. A numerical approach for fractional order Riccati differential equation using B-spline operational matrix. *Fractional Calculus and Applied Analysis*, 18(2):387–399, 2015.
[42] Thibault Jaisson, Mathieu Rosenbaum, et al. Rough fractional diffusions as scaling limits of nearly unstable heavy tailed hawkes processes. *The Annals of Applied Probability*, 26(5):2860–2882, 2016.
[43] Alireza Javaheri. *Inside Volatility Arbitrage: The Secrets of Skewness*, volume 317. John Wiley & Sons, 2011.
[44] Vangipuram Lakshmikantham and Aghalaya S Vatsala. *Generalized Quasilinearization for Nonlinear Problems*, volume 440. Springer Science & Business Media, 2013.
[45] Emmanuel Lépinette and Farshid Mehrdoust. A fractional version of the Heston model with Hurst parameter $H \in (1/2, 1)$. Unpublished results, December 2016.
[46] Alan L Lewis. A simple option formula for general jump-diffusion and other exponential Lévy processes. Unpublished results, 2001.
[47] Alan L Lewis. *Option Valuation Under Stochastic Volatility*. Finance Press, Newport Beach, CA, 2009.
[48] Changpin Li and Chunxing Tao. On the fractional Adams method. *Computers & Mathematics with Applications*, 58(8):1573–1588, 2009.
[49] Changpin Li and Fanhai Zeng. The finite difference methods for fractional ordinary differential equations. *Numerical Functional Analysis and Optimization*, 34(2):149–179, 2013.
[50] Changpin Li and Fanhai Zeng. *Numerical Methods for Fractional Calculus*, volume 24. CRC Press, 2015.
[51] R Lin and Fawang Liu. Fractional high order methods for the nonlinear fractional ordinary differential equation. *Nonlinear Analysis: Theory, Methods & Applications*, 66(4):856–869, 2007.
[52] Alexander Lipton. *Mathematical Methods for Foreign Exchange: A Financial Engineer's Approach*. World Scientific Publishing Company, 2001.
[53] Anna Lischke, Mohsen Zayernouri, and George Em Karniadakis. A Petrov–Galerkin spectral method of linear complexity for fractional multiterm odes on the half line. *SIAM Journal on Scientific Computing*, 39(3):A922–A946, 2017.
[54] Giulia Livieri, Saad Mouti, Andrea Pallavicini, and Mathieu Rosenbaum. Rough volatility: evidence from option prices. *IISE Transactions*, (just-accepted):1–21, 2018.
[55] Richard K Miller and Alan Feldstein. Smoothness of solutions of Volterra integral equations with weakly singular kernels. *SIAM Journal on Mathematical Analysis*, 2(2):242–258, 1971.
[56] Eyal Neuman and Mathieu Rosenbaum. Fractional Brownian motion with zero Hurst parameter: a rough volatility viewpoint. *arXiv preprint arXiv:1711.00427*, 2017.
[57] Igor Podlubny. *Fractional Differential Equations: An Introduction to Fractional Derivatives, Fractional Differential Equations, to Methods of their Solution and Some of Their Applications*, volume 198. Academic Press, 1998.
[58] William Thomas Reid. *Riccati Differential Equations*, volume 86 of *Mathematics in Science and Engineering*. Academic Press, 1972.
[59] V Antony Vijesh. A short note on the quasilinearization method for fractional differential equations. *Numerical Functional Analysis and Optimization*, 37(9):1158–1167, 2016.
[60] Bruce J West. *Physiology, Promiscuity, and Prophecy at the Millennium: A Tale of Tails*. World Scientific, 1999.
[61] M Yarmohammadi, S Javadi, and E Babolian. Spectral iterative method and convergence analysis for solving nonlinear fractional differential equation. *Journal of Computational Physics*, 359:436–450, 2018.
[62] Mohsen Zayernouri. *Spectral and Spectral Element Methods for Fractional PDEs*. PhD thesis, Brown University, 2015.
[63] Mohsen Zayernouri and George Em Karniadakis. Fractional Sturm–Liouville eigen-problems: theory and numerical approximation. *Journal of Computational Physics*, 252:495–517, 2013.
[64] Mohsen Zayernouri and George Em Karniadakis. Exponentially accurate spectral and spectral element methods for fractional ODEs. *Journal of Computational Physics*, 257:460–480, 2014.
[65] Mohsen Zayernouri and George Em Karniadakis. Fractional spectral collocation method. *SIAM Journal on Scientific Computing*, 36(1):A40–A62, 2014.
[66] Fanhai Zeng, Zhiping Mao, and George Em Karniadakis. A generalized spectral collocation method with tunable accuracy for fractional differential equations with end-point singularities. *SIAM Journal on Scientific Computing*, 39(1):A360–A383, 2017.
[67] Fanhai Zeng, Zhongqiang Zhang, and George Em Karniadakis. A generalized spectral collocation method with tunable accuracy for variable-order fractional differential equations. *SIAM Journal on Scientific Computing*, 37(6):A2710–A2732,

2015.

[68] Yuxin Zhang, Hengfei Ding, and Jincai Luo. Fourth-order compact difference schemes for the riemann-liouville and riesz derivatives. In *Abstract and Applied Analysis*, volume 2014. Hindawi, 2014.

[69] Zhongqiang Zhang, Fanhai Zeng, and George Em Karniadakis. Optimal error estimates of spectral Petrov–Galerkin and collocation methods for initial value problems of fractional differential equations. *SIAM Journal on Numerical Analysis*, 53(4):2074–2096, 2015.

[70] Xuan Zhao, Xiaozhe Hu, Wei Cai, and George Em Karniadakis. Adaptive finite element method for fractional differential equations using hierarchical matrices. *Computer Methods in Applied Mechanics and Engineering*, 325:56–76, 2017.